Ion Solid Interactions and their applications

B. Sundaravel

Materials Science Division, IGCAR, Kalpakkam

- **Ion-solid interactions**
- **Some of the applications**
- **Surface morphology caused by MeV Al dimer**
- **Negative Vicinage effect and energy loss of MeV C and O dimers.**

Ion-solid interactions

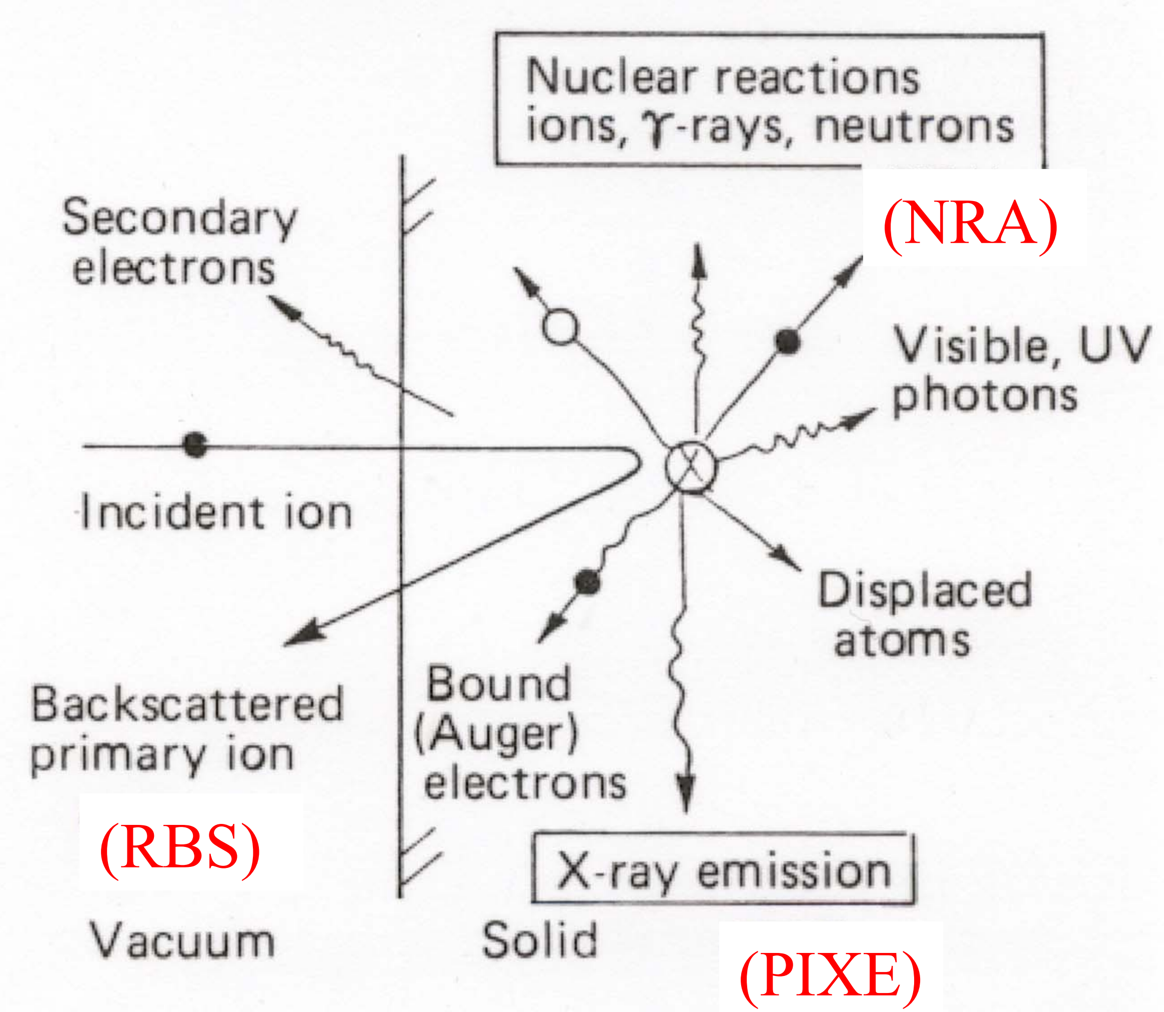

(NRA)

(RBS)

(PIXE)

Ion beam analysis

- **RBS:** Thickness and composition of thin films,Multi-elemental concentration depth profile
- **Channeling:** Crystalline quality, mosaic spread, polarity, mixed phases, Lattice location of impurity atoms, Type and density of defects, polarity, In-plane orientation, tetragonal strain and tilt of epitaxial layers on crystalline substrates, Structural phase transitions, Surface reconstructions under UHV
- **PIXE:** Impurity atom detection at ppm level, Multielemental concentration determination
- **ERDA:** Depth profile of light target atoms like Hydrogen
- **NRA:** Isotope selective concentration depth profile

1.7 MV Tandetron Accelerator at IGCAR, Kalpakkam

Ions of almost all elements in the periodic table

Energy → 0.3 MeV to 1.7(1+q) MeV

Beam Current → few μA

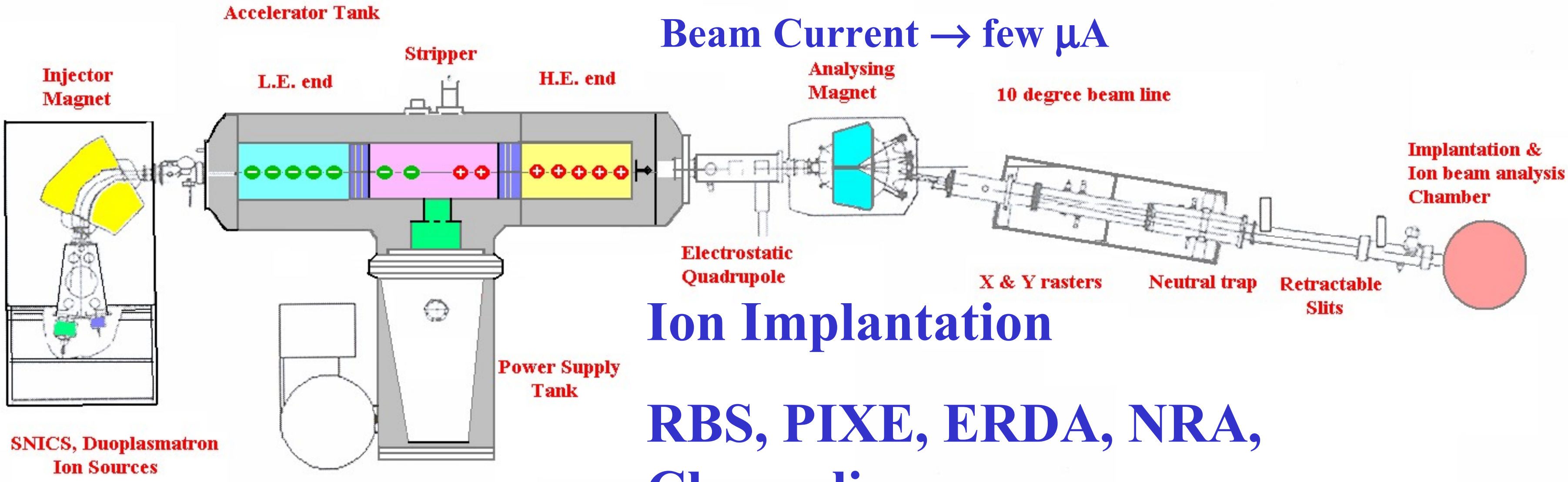

Ion Implantation

RBS, PIXE, ERDA, NRA, Channeling

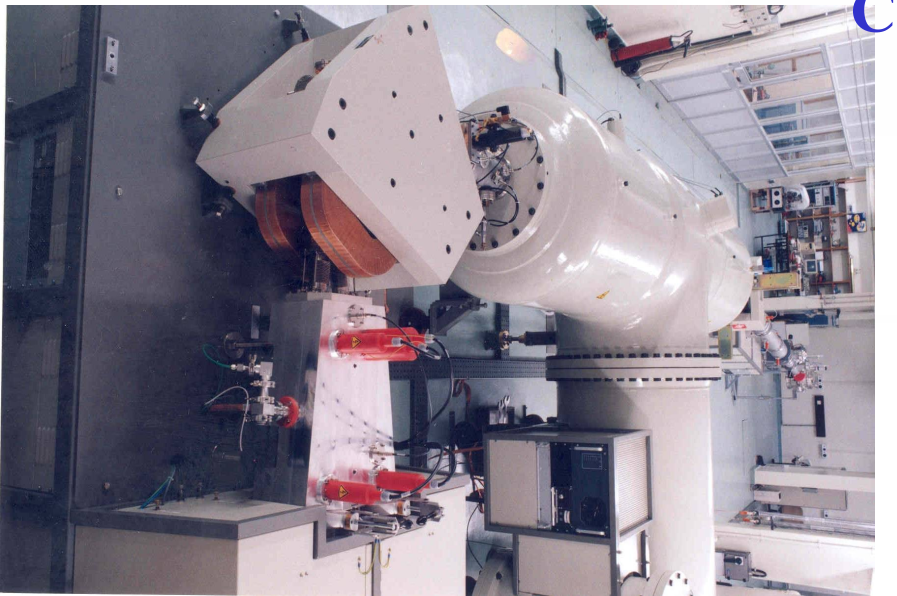

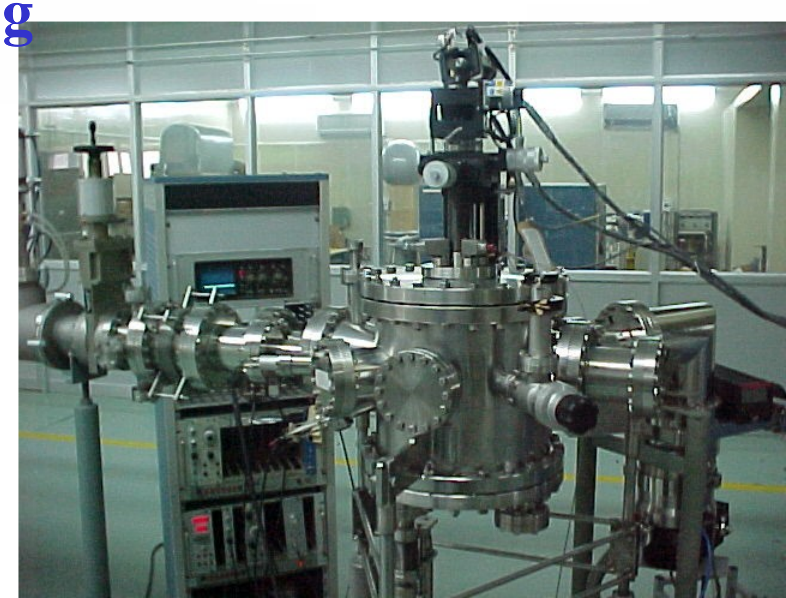

Applications of ion implantation

- Doping to change the electronic and material properties
- Good controllability of doping levels and spatial distribution of impurity
- Improvement of hardness and corrosion resistance
- Producing highly non-equilibrium states with novel material properties
- Ion-beam enhanced diffusion
- Ion-beam enhanced segregation
- Ion-beam mixing
- Ion-beam induced crystallization
- Ion-beam synthesis
- Ion-beam assisted deposition
- Sputtering
- Gettering
- Ion beam Smart-cut
- Nano capillaries with single ion impacts
- Fabrication of an array of sharp micro tips or aligned wires
- Focused ion beams, to produce sub-micron-scale features on solid substrates (ion beam sculpting) and doping in microstructures

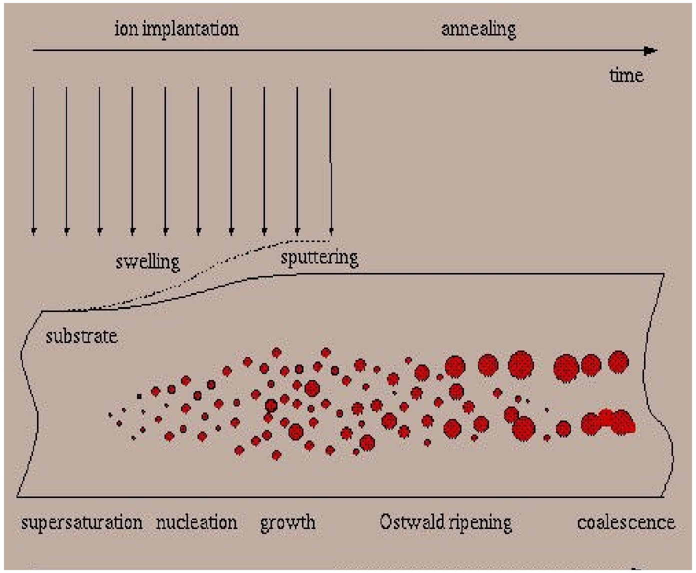

Microstructures with focussed ion beam

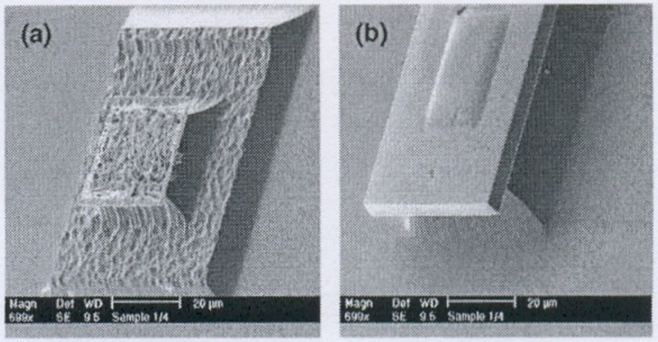

Fig. 3. (a) 100×100 μm² structures irradiated with 1.2×10^{15} cm^{-2} with inner region of 20×20 μm² irradiated with 2.4×10^{15} cm^{-2}, created using (a) OMDAQ and (b) IONSCAN.

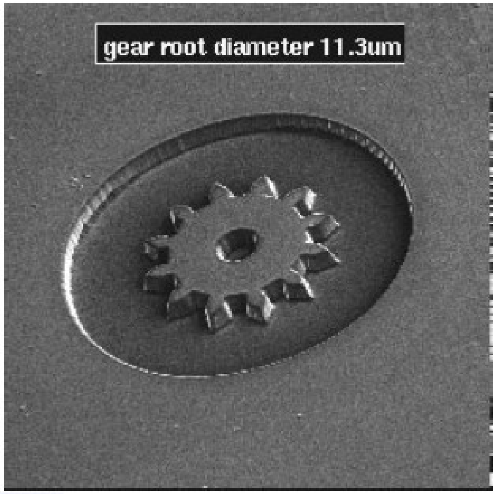

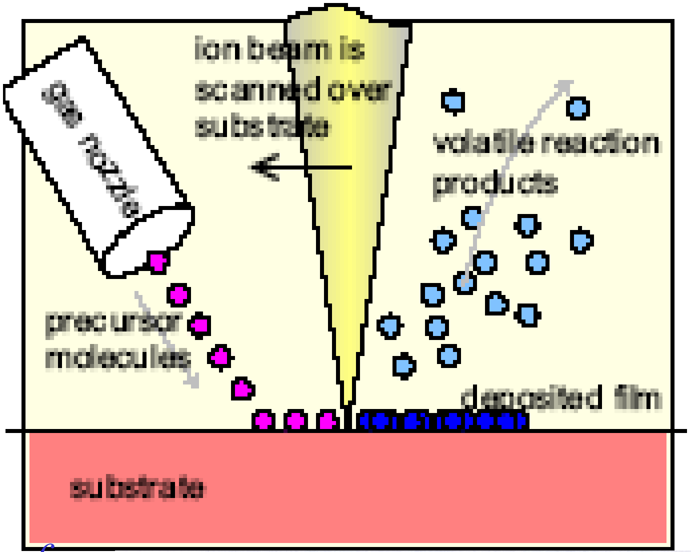

Teo et al NIMB 222 (2004) 513

Fu et al, Int. J. Adv. Manuf. Technol. 16 (2000) 600

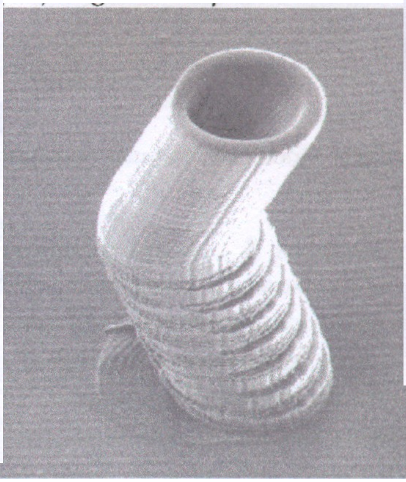

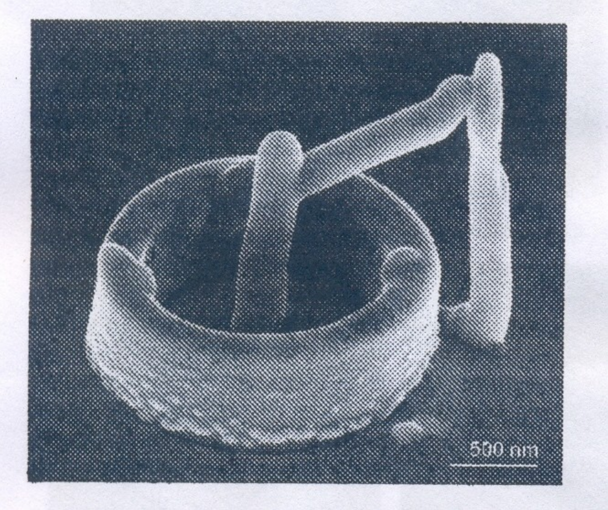

Reyntjens,et al, J. Micromech. Microeng. 11 (2001) 287

Energy loss

The incident ions lose energy by two processes:

2. **Electronic Energy loss (exitation of target electrons)**
3. **Nuclear energy loss (hard sphere collision)**

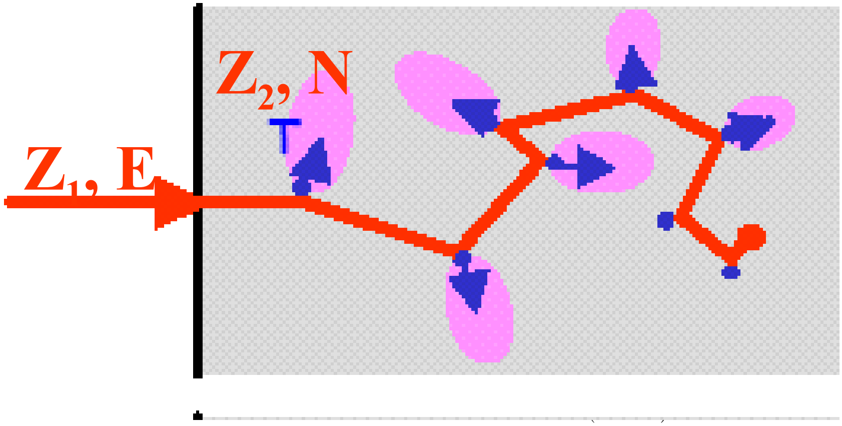

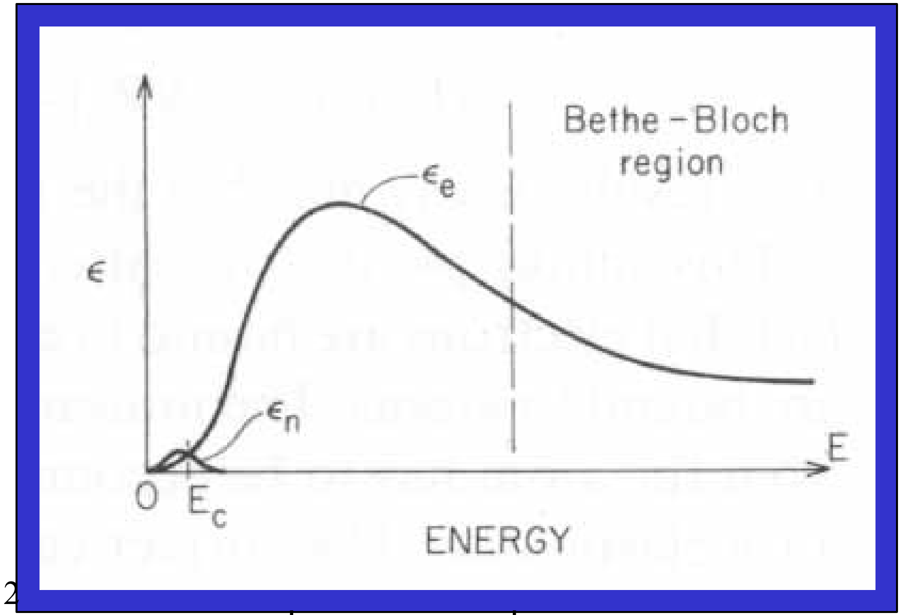

$$-\varepsilon_e = -\frac{1}{N}\frac{dE}{dX} = \frac{4\pi z_1^2 z_2 e^4}{m v_0^2}\ln\left(\frac{b_{max}}{b_{min}}\right) \propto (z_1 e)^2$$

$$\varepsilon = \left.\frac{1}{N}\frac{dE}{dx}\right|_e + \left.\frac{1}{N}\frac{dE}{dx}\right|_n$$

$$\frac{\varepsilon_e}{\varepsilon_n} \approx \frac{M_2}{Z_2 m_e} \approx 3600$$

$$\varepsilon = A_0 + A_1E^1 + A_2E^2 + \ldots + A_5E^5$$

Energy Straggling

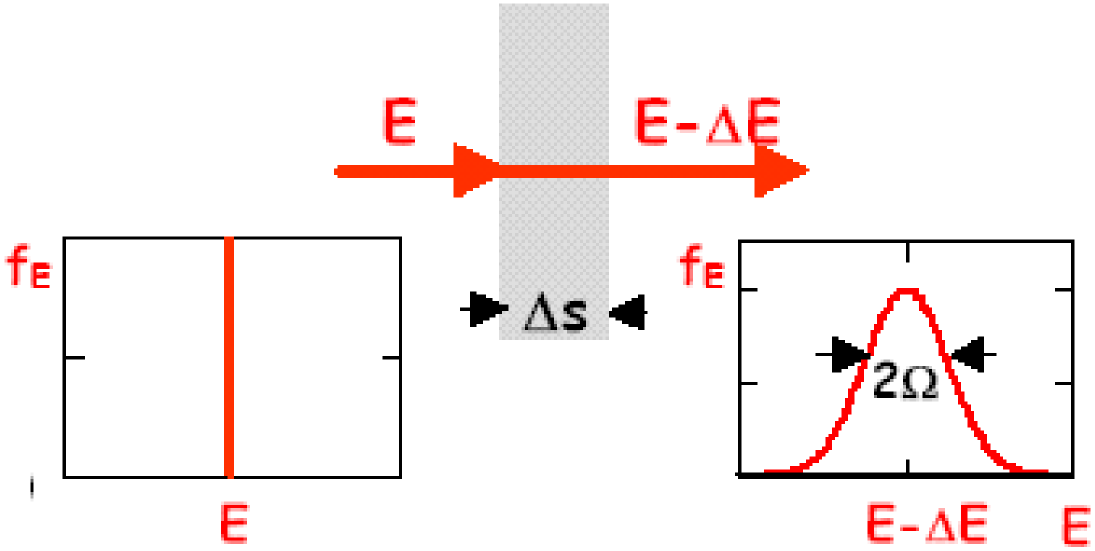

$$\frac{\Omega_e^2}{n\Delta s} = \frac{4\pi e^4 Z_1^2 Z_2}{(4\pi\varepsilon_0)^2}$$

Limits Depth resolution in Ion Beam Analysis

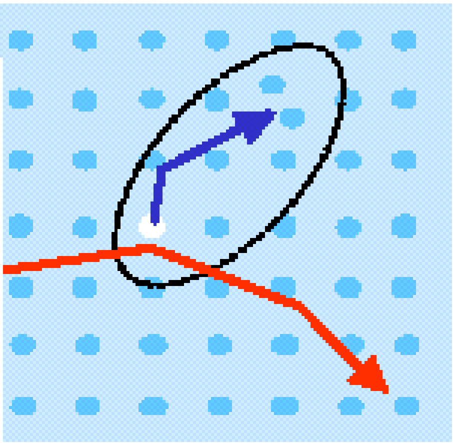

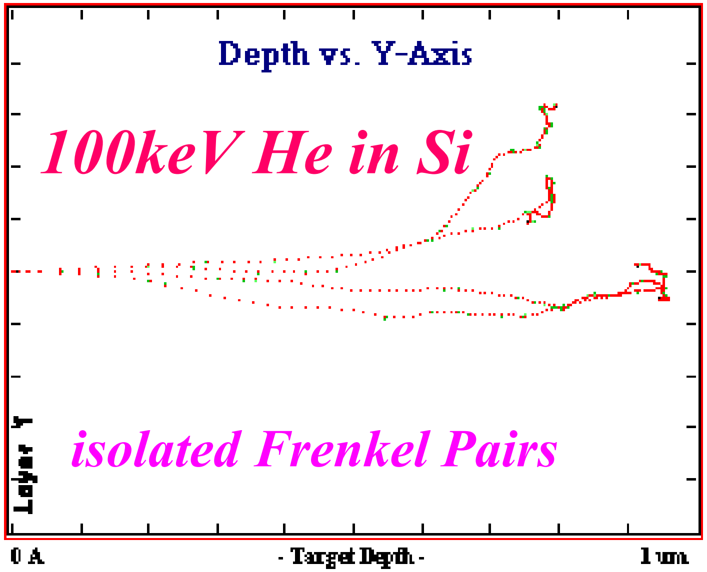

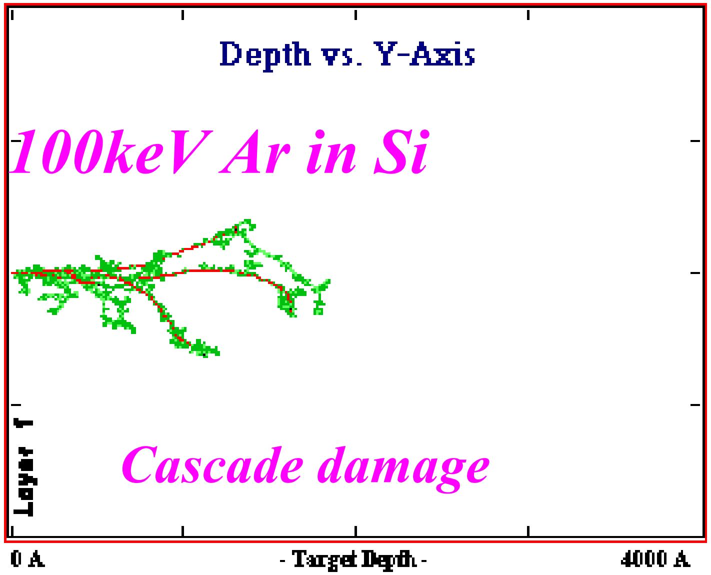

Time (sec)	Event	Result
10^{-18}	Energy Transfer	PKA
10^{-13}	Displacement	Displacement of atoms
10^{-11}	Energy Dissipation	Stable Frenkel pairs
10^{-8}	Defect reactions	migration recombination, clustering

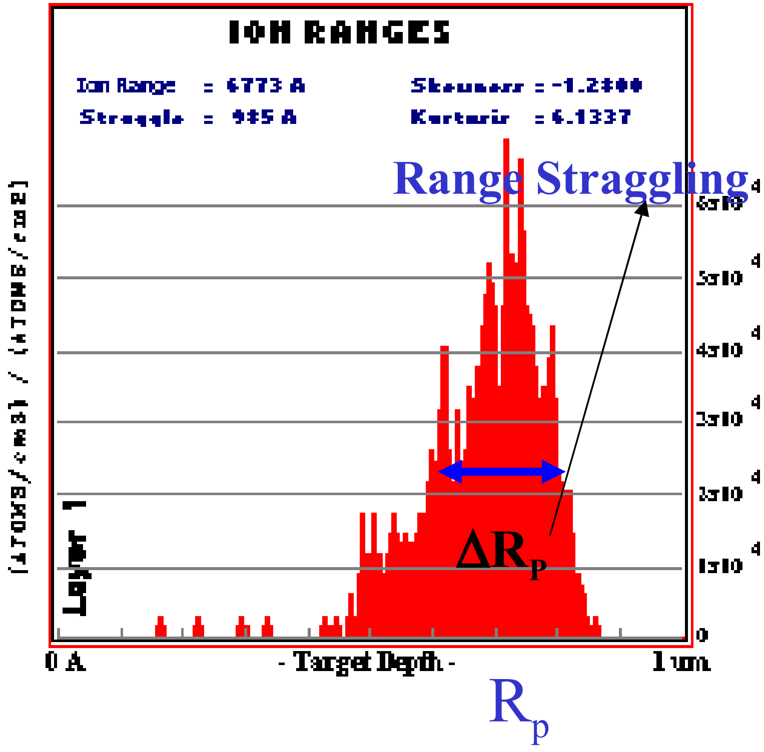

ENERGY DEPOSITION

- 1MeV N^+in Fe

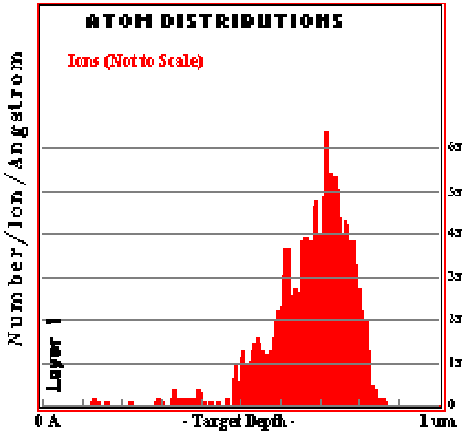

Ion Range

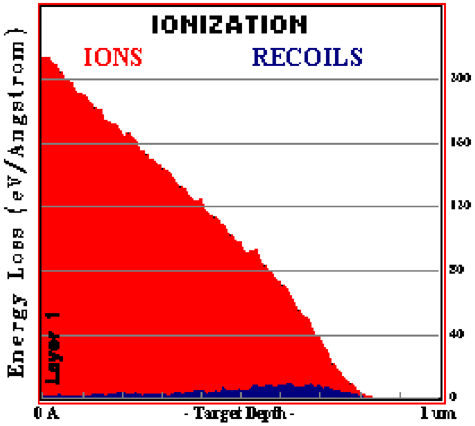

Ionization $(dE/dx)_e$

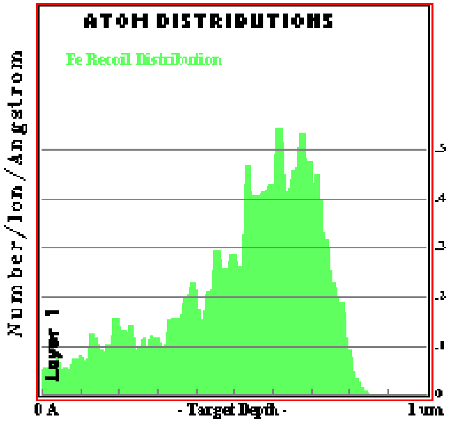

Target Displacements $(dE/dE)_n$

- Defect Production

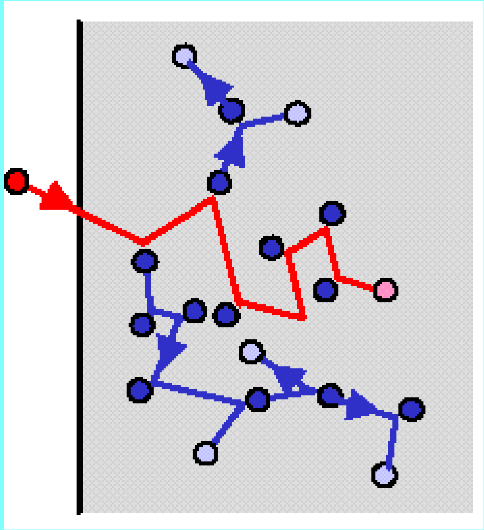

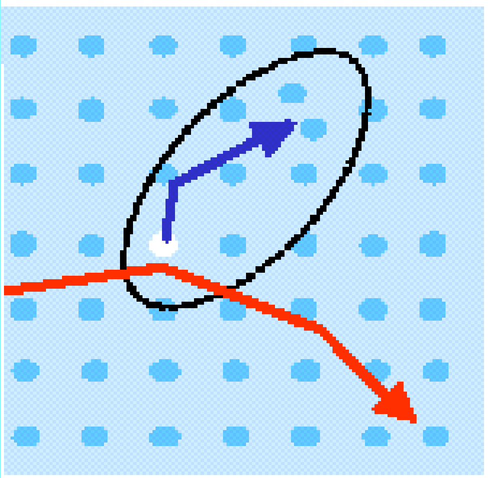

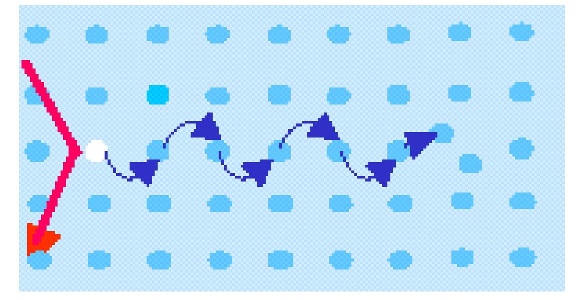

Replacement Collision Sequence

- Target atom gets displaced to a n interstitial site producing a vacancy and interstitial defect

SPUTTERING

- When a collision cascade intersects the surface, sufficient energy can be transferred to a surface atom to overcome its binding to the surface.

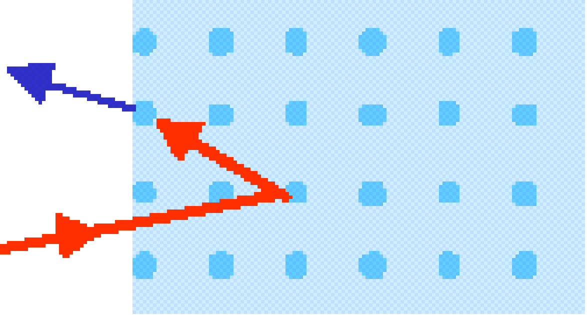

Light-ion sputtering event in the single-collision regime.

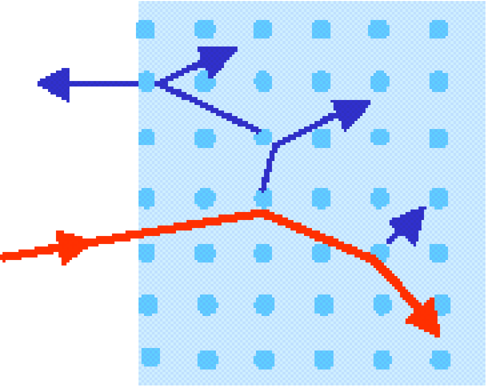

Linear cascade regime.

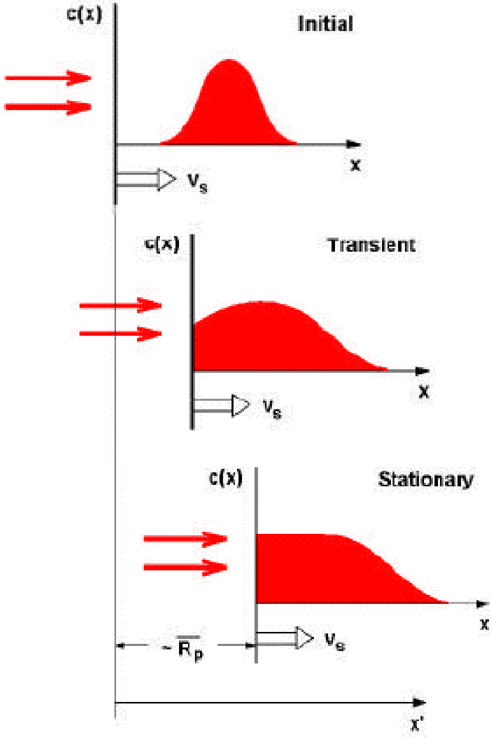

IMPLANTATION PROFILES

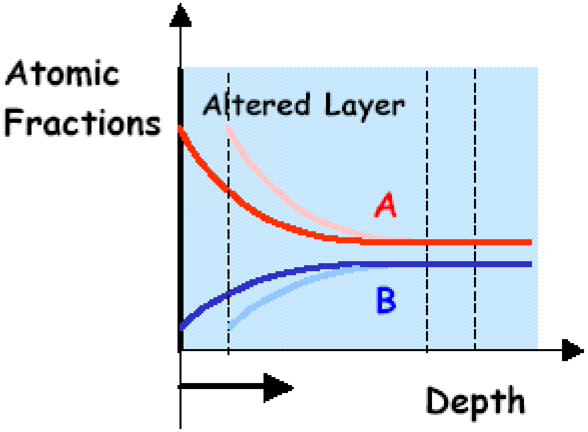

Preferential Sputtering effects in alloys

Kinematic Factor and crosssection for backscattering and recoil

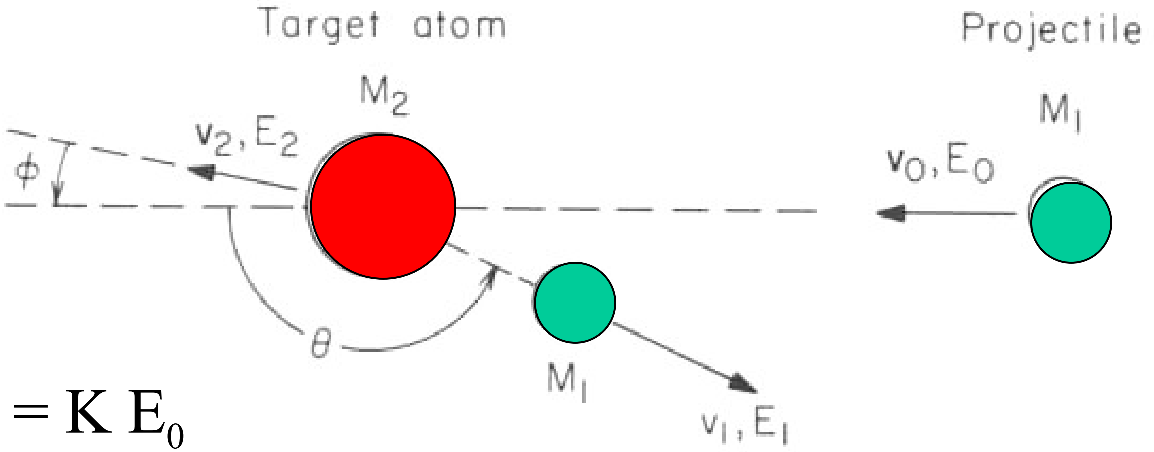

$$E_1 = K\,E_0$$

From the laws of conservation of energy and momentum,

$$K = \left\{ \frac{(M_1/M_2)\cos\theta + (1 - (M_1/M_2)^2 \sin^2\theta)^{1/2}}{1 + (M_1/M_2)} \right\}^2 \qquad K = \frac{2M_1M_2\cos^2\varphi}{(M_1 + M_2)^2}$$

Yield $Y = Q\,\Omega\,\sigma\,N\,t$

$$Y_r(E_d) = \frac{QN_r(x)\sigma_r(E_o',\varphi)\Omega\,\delta E_d}{\cos\Theta_1 dE_d/dx}$$

$$\sigma = \left(\frac{z_1z_2e^2}{2E}\right)^2 \frac{1}{\sin^4\frac{\vartheta}{2}}$$

$$\sigma_r(E_o',\varphi) = \frac{[Z_1Z_2e^2(M_1 + M_2)]^2}{[2M_2E_o']^2\cos^3\varphi}$$

RBS and channeling

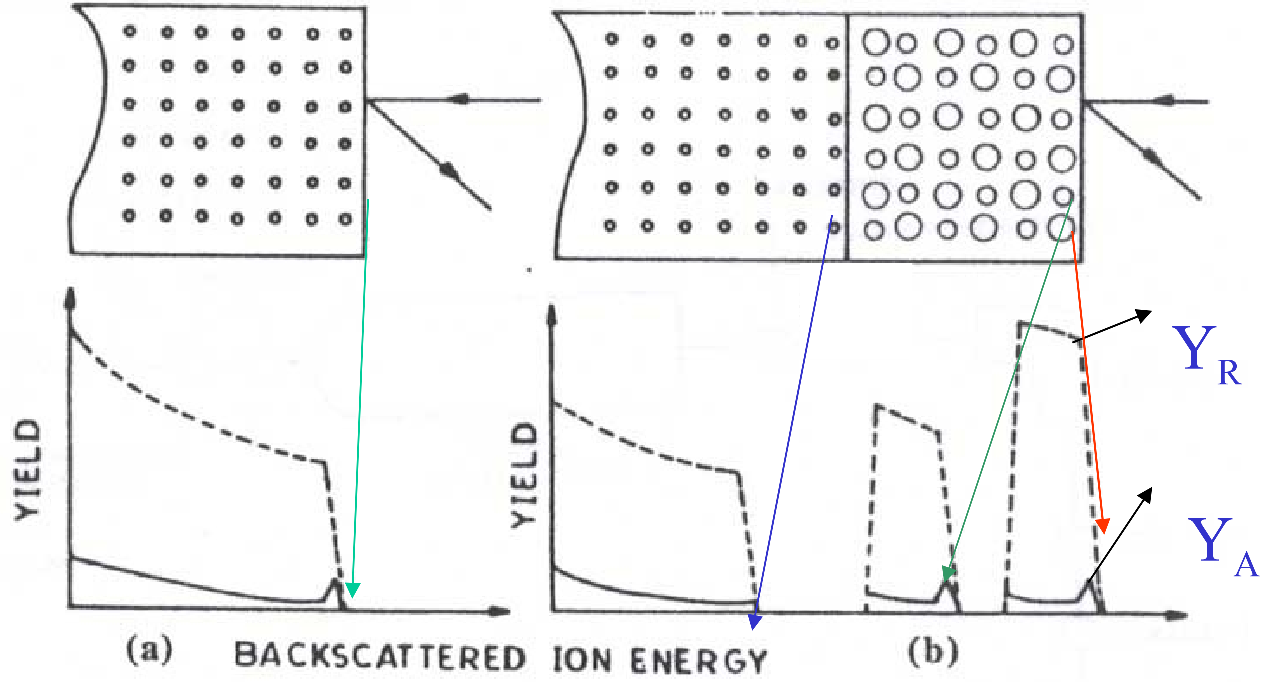

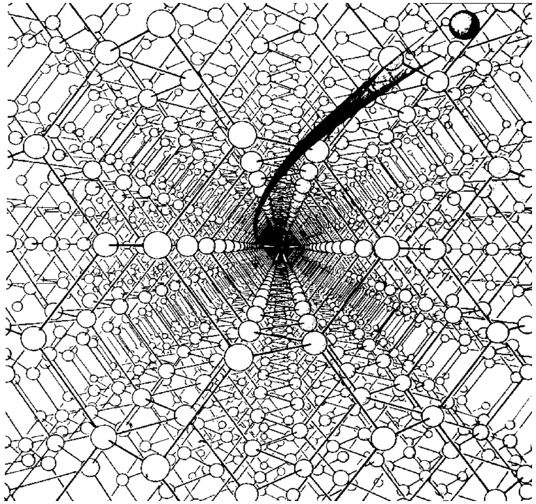

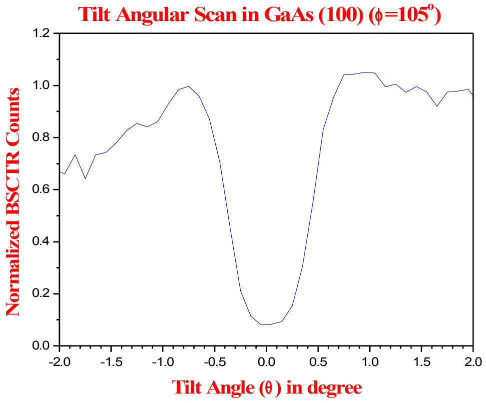

$$\chi_{min}=Y_A/Y_R$$

Amorphisation in Carbon implanted GaAs(100)

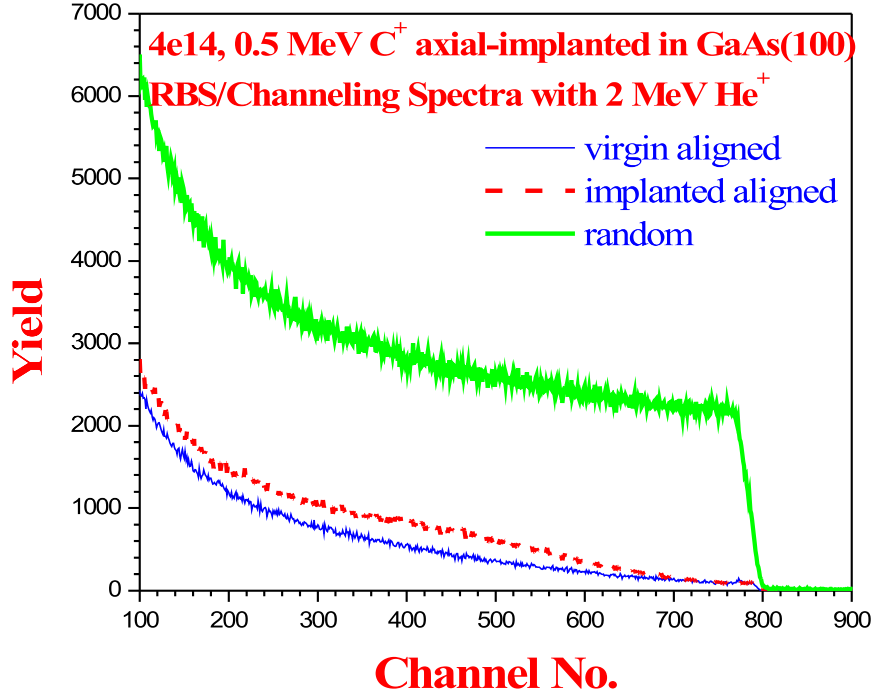

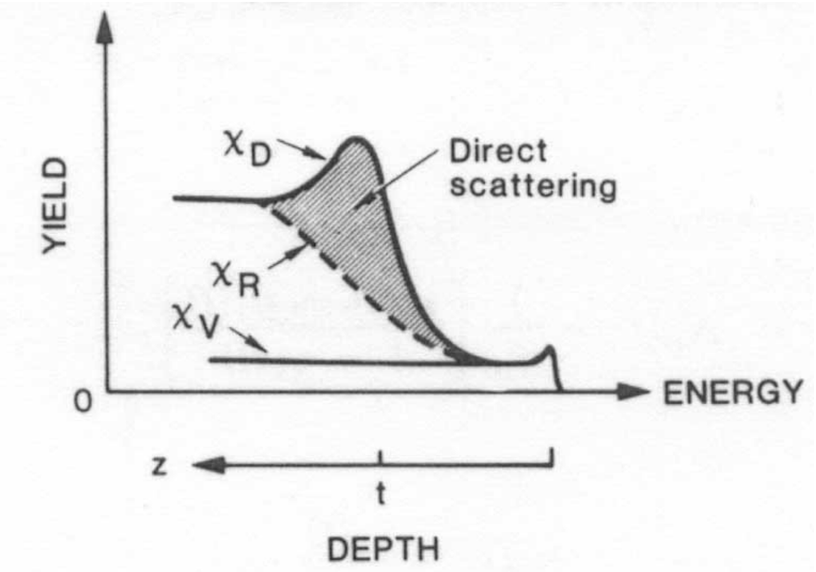

K. Suresh et al, Rev. of Sci. Instr. 75 (2004) 4891

Ion beam induced crystallization in 1MeV Si$^+$ implanted Ag/Si(111)

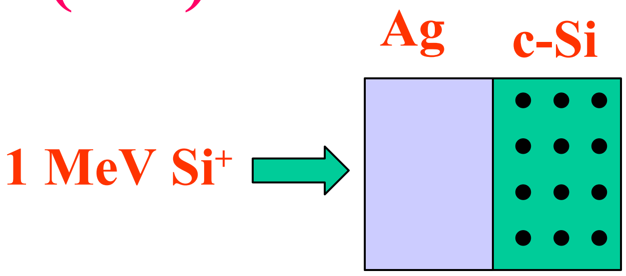

Ag

c-Si

1 MeV Si$^+$

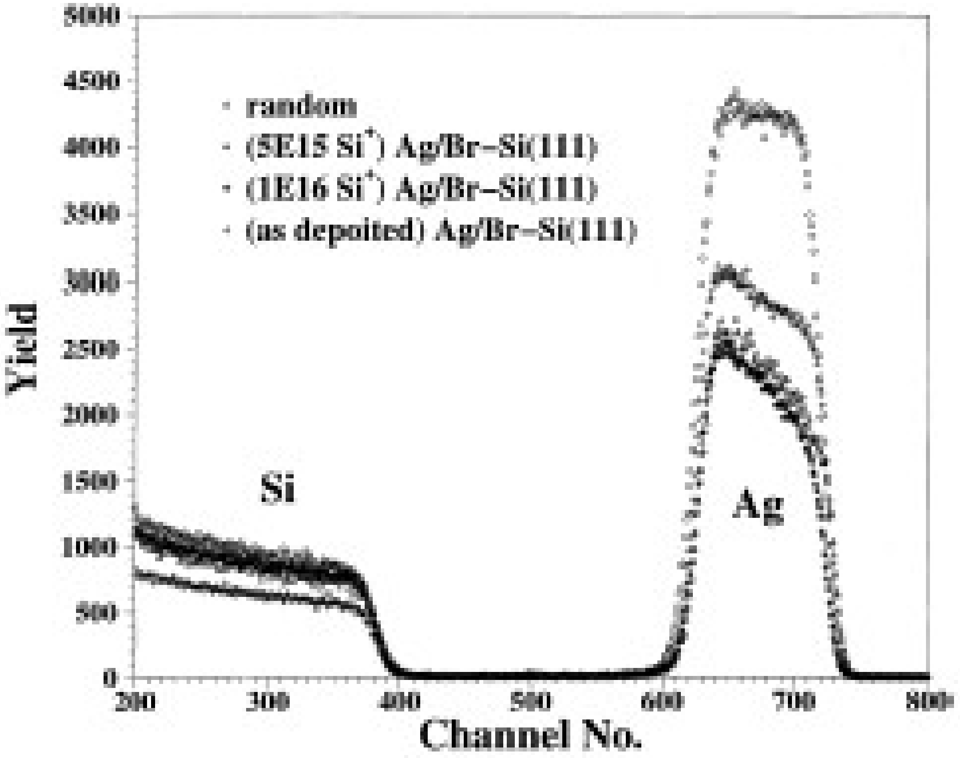

B. Sundaravel et al, Nucl. Instr. and Meth. B 156 (1999) 130.

Radiation enhanced diffusion and segregation

Fe depth profile in 40kV Fe implanted Ge for various doses obtained from AES (Fe$_{LMM}$)

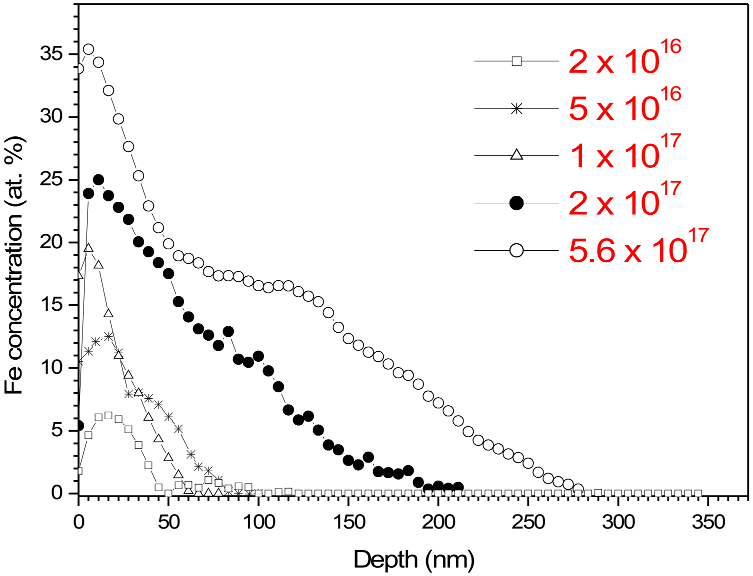

Rp=31 nm (TRIM value), Expt: > 6Rp

Diffusion is through defects like vacancies or interstials. Irradiation Produces large concentration of Defects causing Enhancement in Atomic Mobility

R. Venugopal, B. Sundaravel et al, Appl. Surf. Sci. 185, 60 (2001): J. Appl. Phys. 91, 1410 (2002)

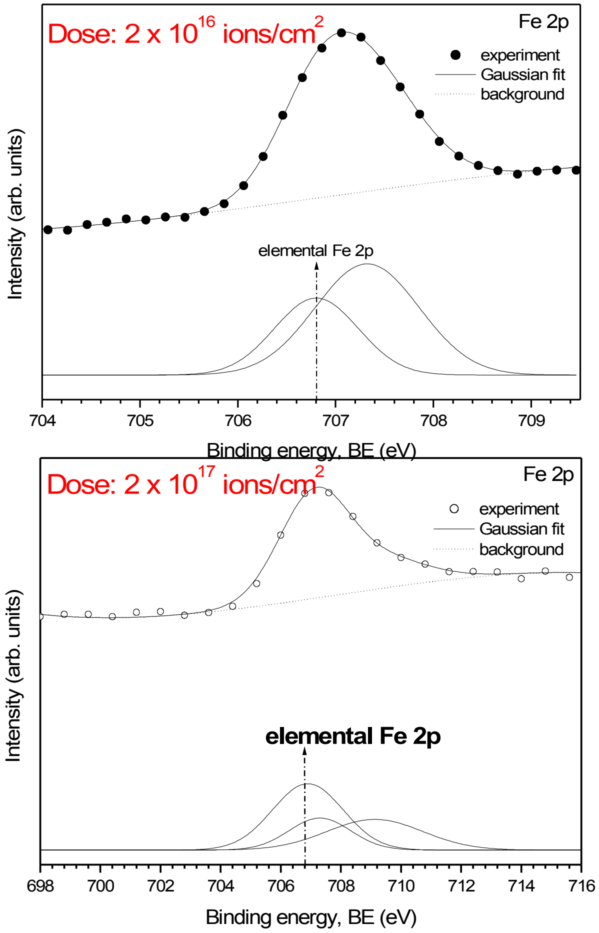

Fe 2p XPS data

Dominant phase: Fe-Ge (lower dose)

Fe (higher dose)

ION BEAM MIXING in Ag/Fe/Ag/Fe multilayer

In an inhomogeneous multicomponent substance, the relocation of atoms due to ion knockon and collision cascades results in "mixing" of the atoms.

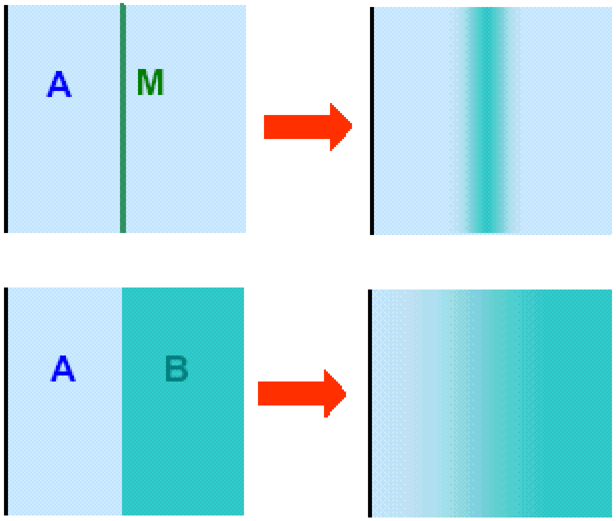

Intermixed layer thickness 1.3 nm

Interfacial Free Energy – 35 kJ/mole

Heat of Mixing of a Random Mixture of $Fe_{30}Ag_{70}$ – 25 kJ/mole

Metastable $Fe_{30}Ag_{70}$ Random Alloy

Amirthapandian *et al.*, *Phys. Rev. B* *69 (2004) 165411*

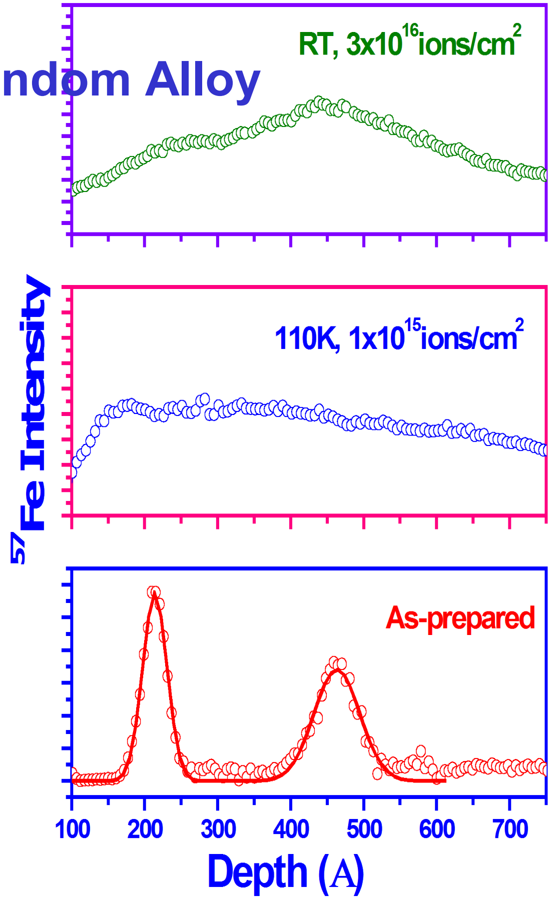

- **Reduction of strain, dislocation density in ion beam mixed $In_{0.18}Ga_{0.82}As$/GaAs(100) upon irradiation with 150 MeV Ag^{12+} ions.** *S. Damodharan et al, NIMB 244 (2006) 174*

Enhanced Gettering of Au in Ge dimer implanted Si

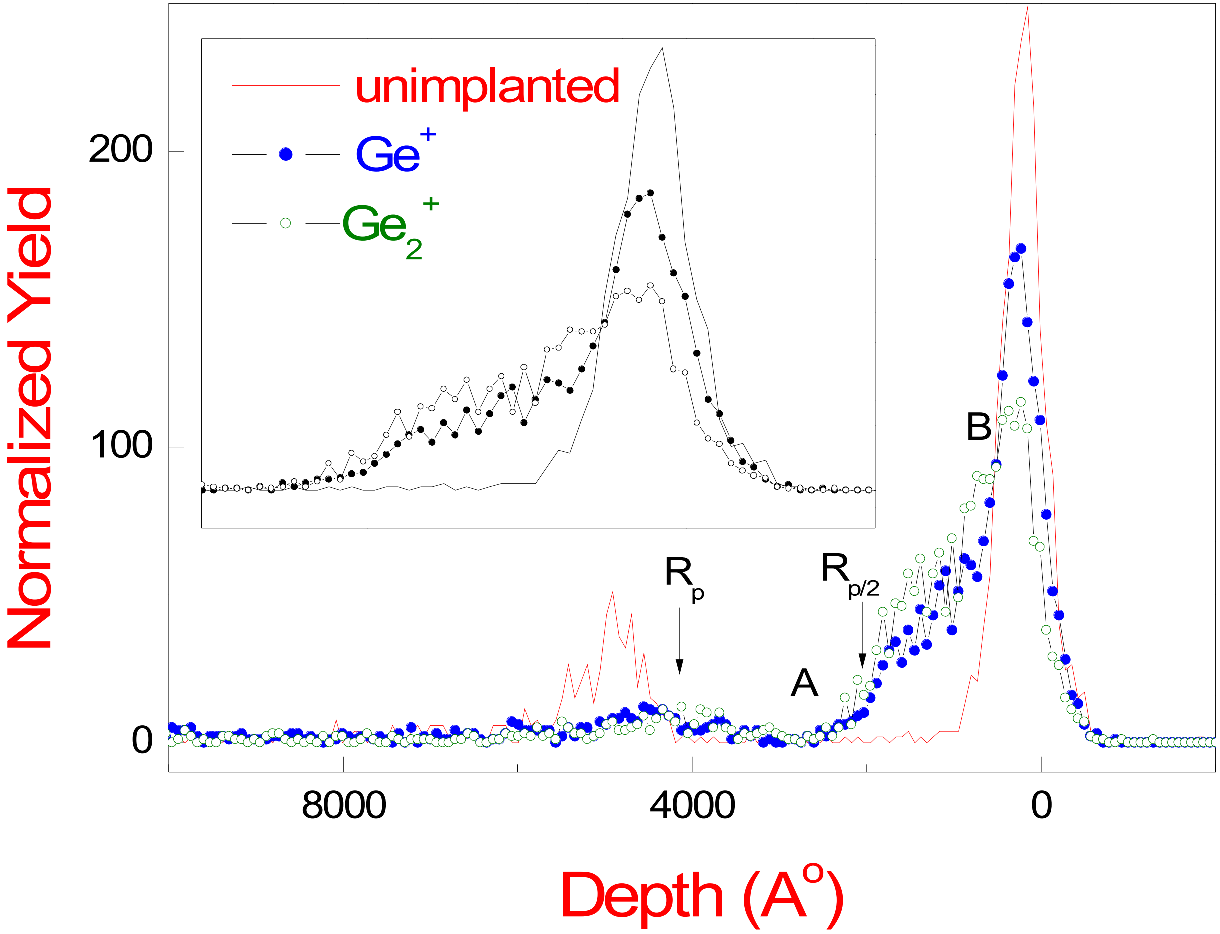

Christopher David et al (communicated)

ION BEAM SYNTHESIS OF NANOSTRUCTURES

EMBEDDED NANO CLUSTERS IN DIELECTRICS

- **OPTICAL PROPERTIES**
- **Au, Ag,Cu & Ge CLUSTERS IN SiO_2,, GLASS &Al_2O_3**

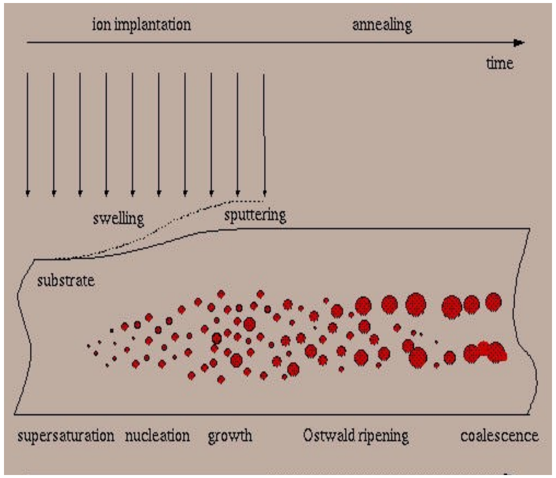

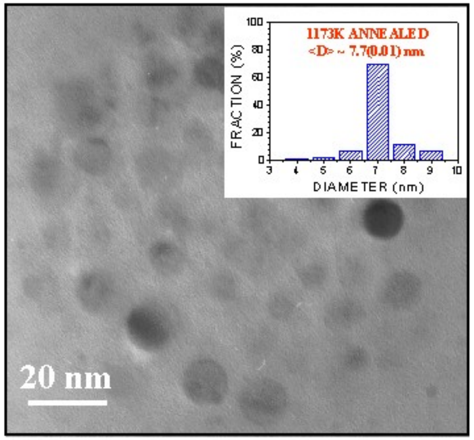

Au NANOCLUSTERS IN SILICA

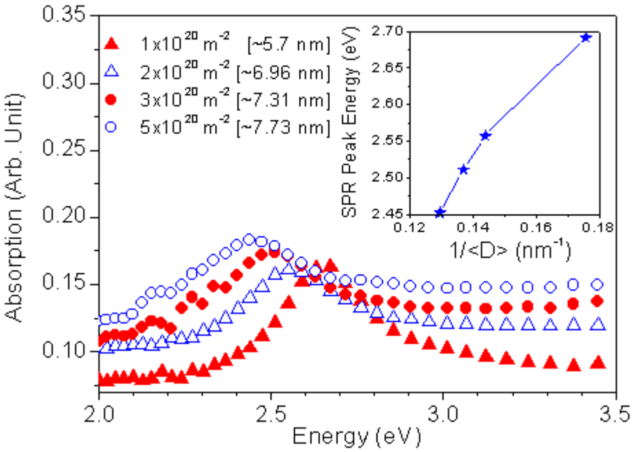

SIZE EFFECTS IN OPTICAL PROPERTIES

S. Dhara etal Chem. Phys. Lett. 370 (2003) 254

PL-FROM Ag NANO CLUSTERS IN GLASS

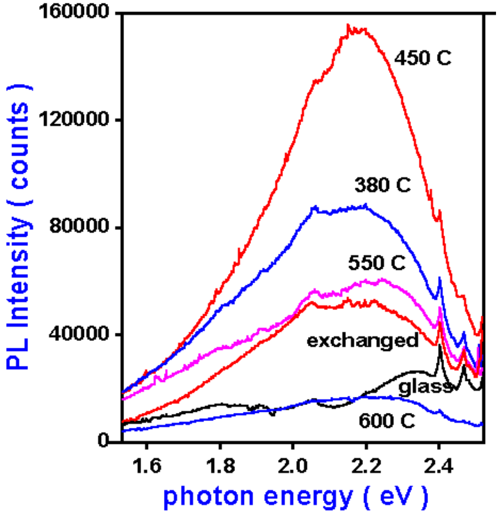

Earlier Studies PL- Ag ions

We have shown through XPS studies that the PL emission is from AgO

P. Ganguly et al. PRL 94 (2005) 047403.

RBS/channeling in Si/$CoSi_2$/Si(111) prepared by Ion Beam Synthesis

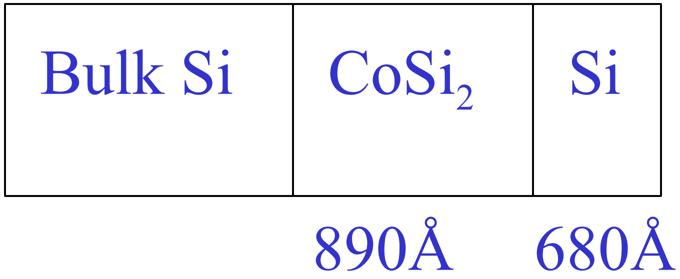

Bulk Si

$CoSi_2$

Si

890Å 680Å

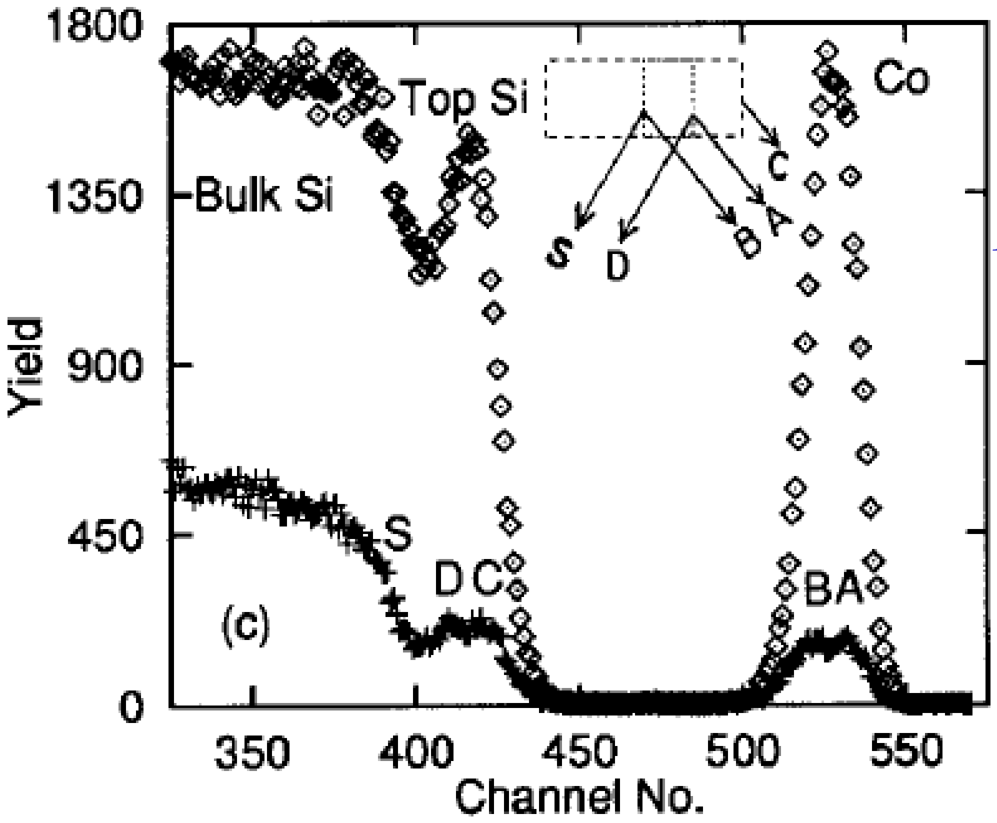

P. V. Satyam et al, Philos. Mag. Lett. 73, (1996) 309.

Surface Modification caused by Ion beams

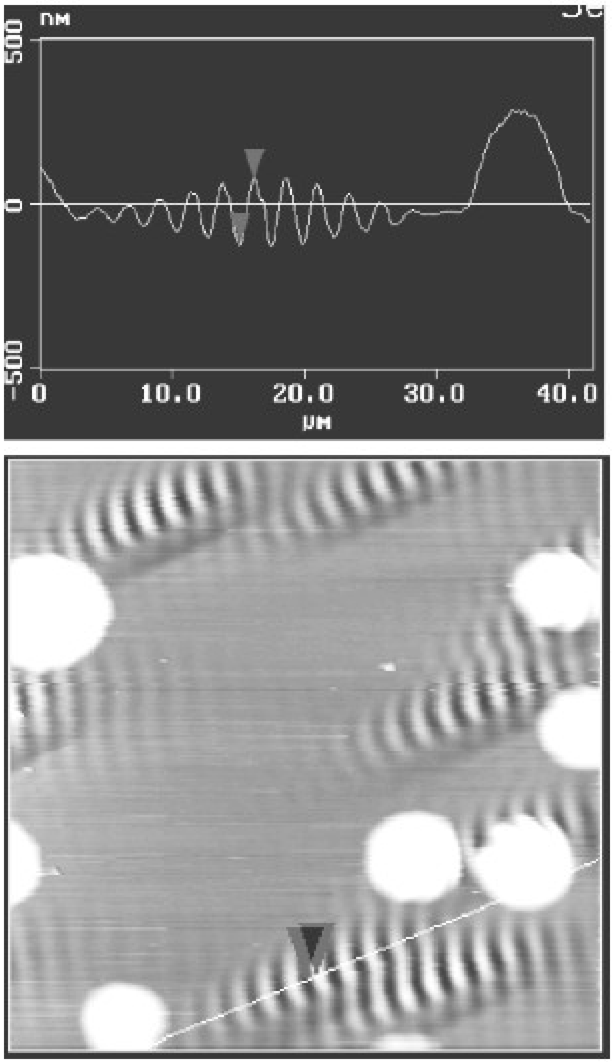

Fig. 6. A plan view (bottom) AFM micrograph showing islands and ripple formation near the islands, along with a cross-sectional view (top) of undulations along the line in the bottom micrograph.

B. Rout et al, NIMB 181 (2001) 268

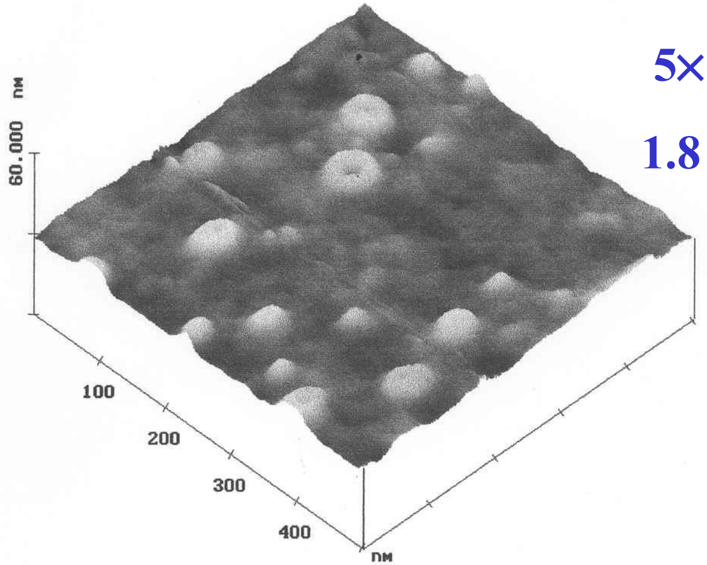

5×10^9 ions/cm^2

1.8 crater/ion

Single Ion Impacts of 0.5 MeV Ge on 40nm SiO$_2$/Si(100)

Hillocks formed by Pb implantation in Quartz

Fig. 2. AFM (1 μm × 1 μm) of a specimen bombarded by 0.73 GeV Pb [illegible] cm^{-2}, vertical scale 8 nm/division).

I.H. Wilson et al, NIMB 118 (1996) 473

Wilson’s model

I. H. Wilson et al, Phys. Rev. B38 (1988) 8444.

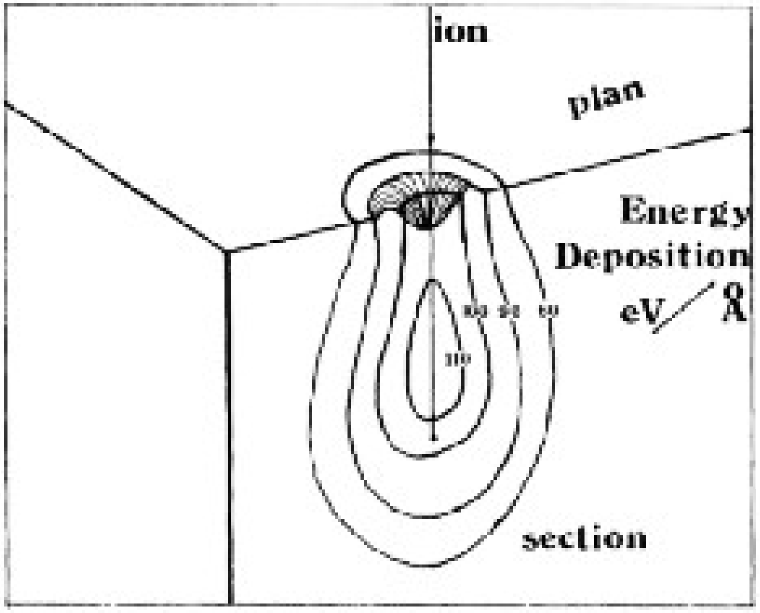

Crater width is of the lateral extent of the nuclear energy deposition.

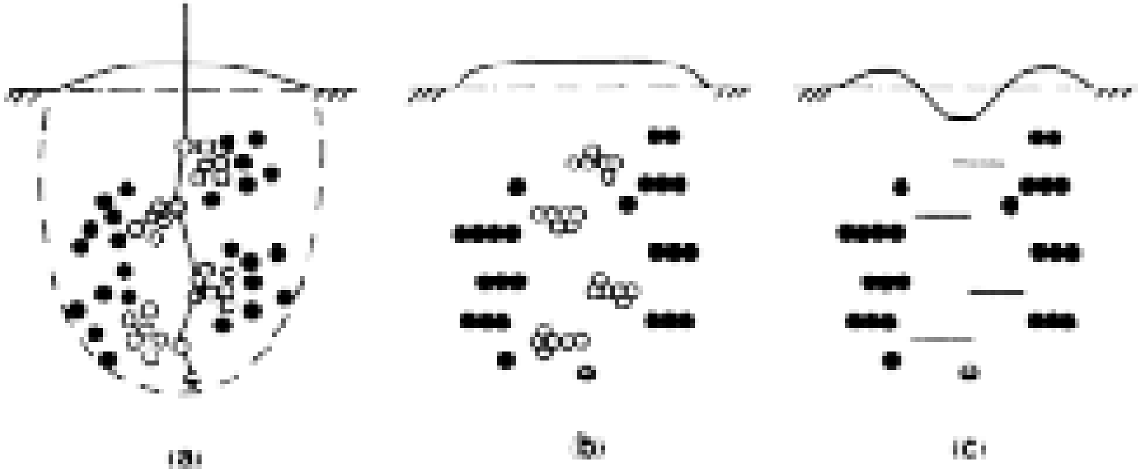

(a) Creation of vacancies & interstials (b) vacancy clusters & interstial planes (c)collapse of the surface to fill in vacancies, crater & rim.

The atomic rearrangements following the cascade due to nuclear energy deposition are responsible for the formation of the craters

Ferroelectric Triglycine Sulphate irradiated with 0.5 MeV Al^+

Ferroelectric ↔ Paraelectric

T_c=49°C

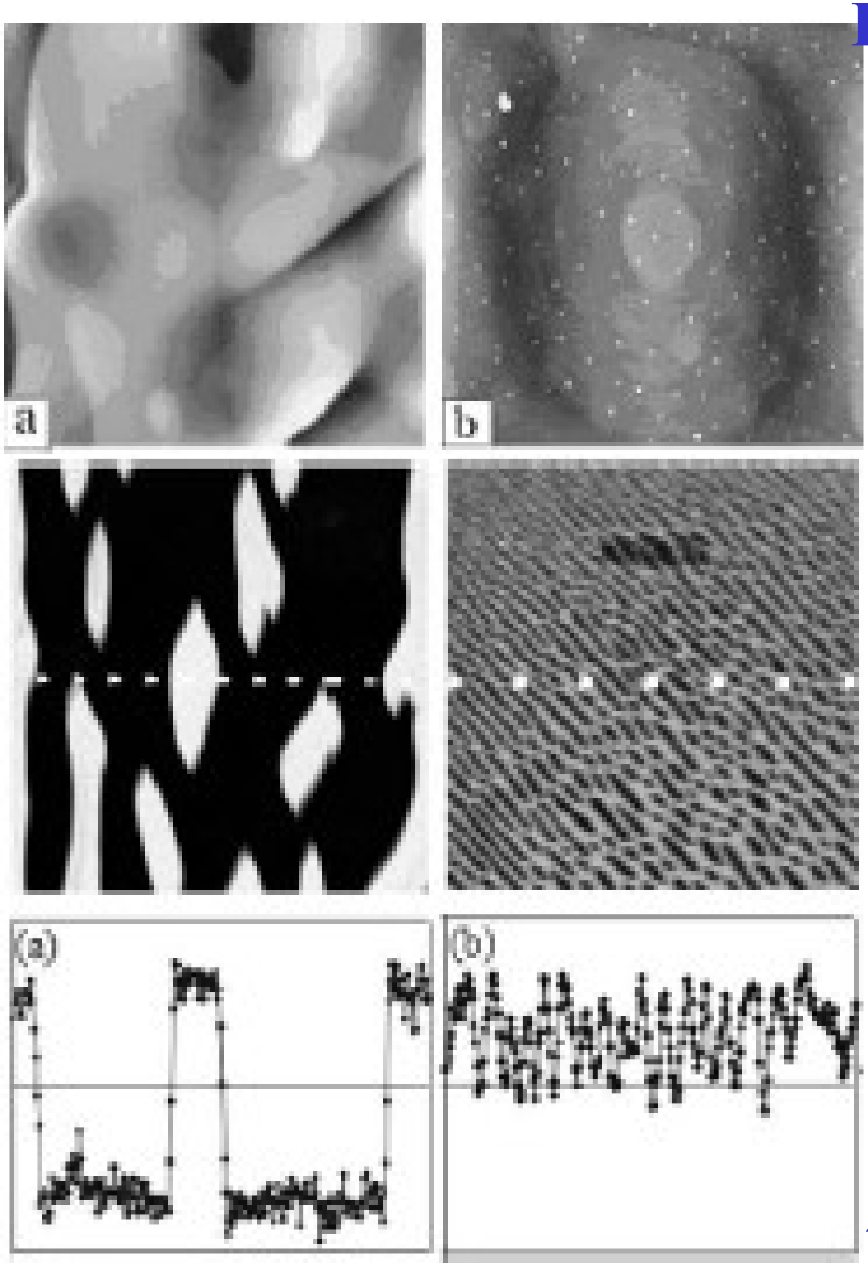

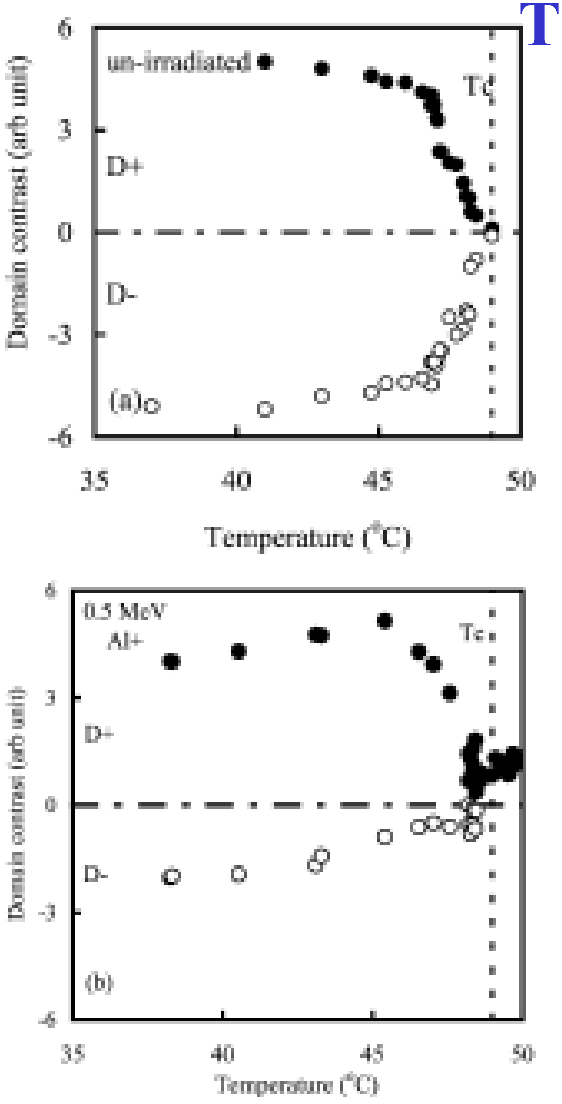

Z. Xie et al, Phys. Lett. A 309 (2003) 121

Electroactive polymers as artificial muscles

- **Two orders of increase in electrostrictive coefficient upon 3 MeV proton irradiation in Copolymer (80% vinylidene fluoride+20%trifluoroethylene)**
- **There is decrease in hysterisis showing that material has become relaxor ferroelectric**
- **XRD shows an additional peak at a lower 2θ corresponding to a paraelectric phase** *S.T. Lau et al, Ferroelectrics 273 (2002) 9.*

FIGURE 1: Grand challenge for the development
EAP actuated robotics

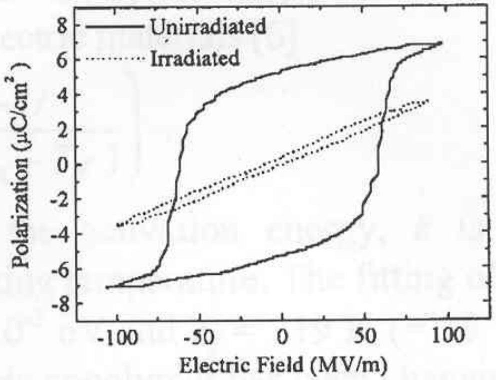

Fig. 1 Polarization hysteresis loops for unirradiated and irradiated copolymers.

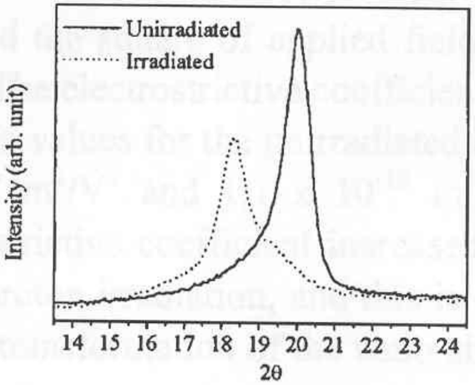

Fig. 3 XRD patterns for unirradiated and irradiated copolymers.

CHARGED PARTICLE SIMULATION OF FAST NEUTRON DAMAGE

FAST REACTOR STRUCTURAL MATERIALS → **DISPLACEMENT DAMAGE** → **VOID SWELLING** Dimensional Changes

Intense Neutron flux

VOIDS → **VACANCY CLUSTERS** →

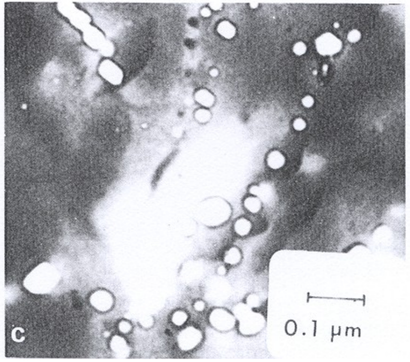

ION SIMULATION STUDIES

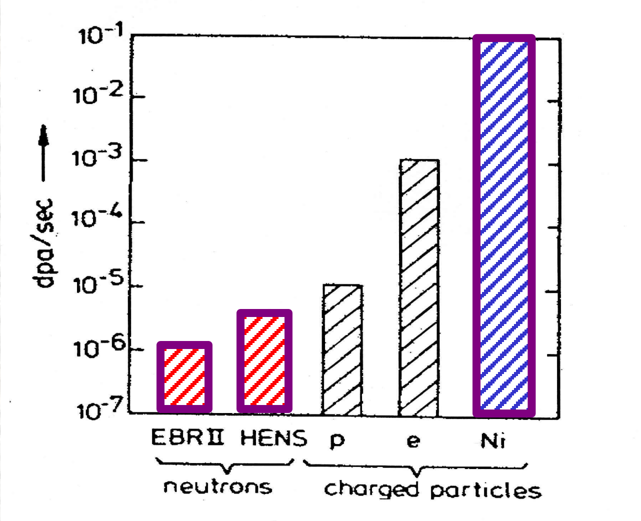

5MeV Nickel Ions are used for Simulating Neutron Damage

Screening of Materials

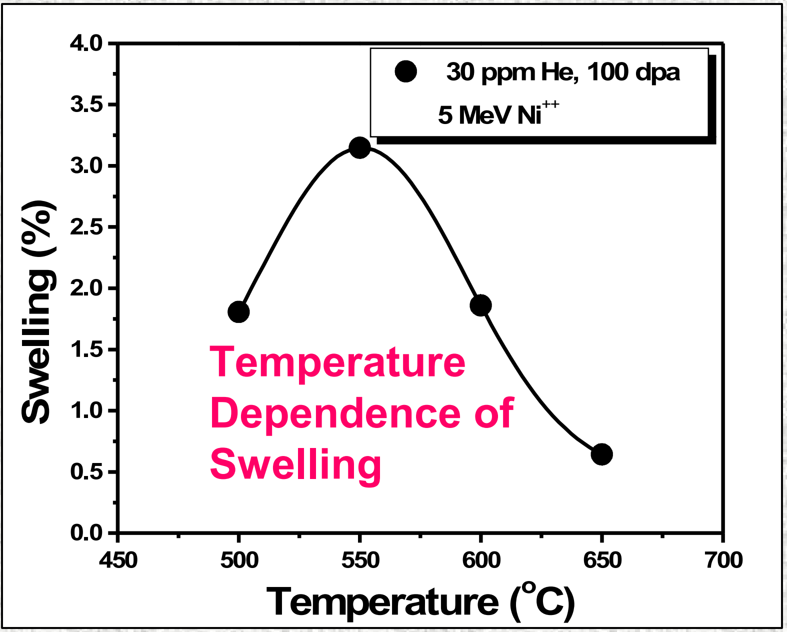

- **Cluster ion beam has a lot of applications: ultra-shallow junctions (less than 7 nm in Si at 2 keV) very high-rate sputtering (more than 2 orders higher than monomer ions) atomic scale smoothing of surfaces (roughness < 0.2 nm) reactive thin film formation at low substrate temperatures *I. Yamada, Nucl. Instr. Meth. B 148 (1999) 1.***
- **Cluster ions deposit extremely high density of electronic energy. *H. Dammak et al , Phys. Rev. Lett. 74 (1995) 1135.***
- **There is non-linear effect in cluster-solid interaction and it has been investigated in various cluster impact phenomena such as damage production, energy loss and sputtering. *P. Sigmund et al, Nucl. Inst. and Meth. B 112 (1996) 1.***
- **Craters have also been observed in cluster ion implantation at low doses.**
- **Thermal Spike Model: Constant diameter of craters at different energies. *K. L. Merkle et al, Phil. Mag. A 44 (1981) 741***
- ***Collision Cascade overlap model: Only some of the craters are stable T. Aoki et al, Nucl. Instr. And Meth B 153 (1999) 264: J. Liu et al, Nucl. Instr. Meth. B 190 (2002) 787.***
- ***Pressure pulse, shock wave, Coulomb explosion, M. Dobeli at al, Nucl. Instr. and Meth. B 143 (1998) 503.***

Single Ion impacts

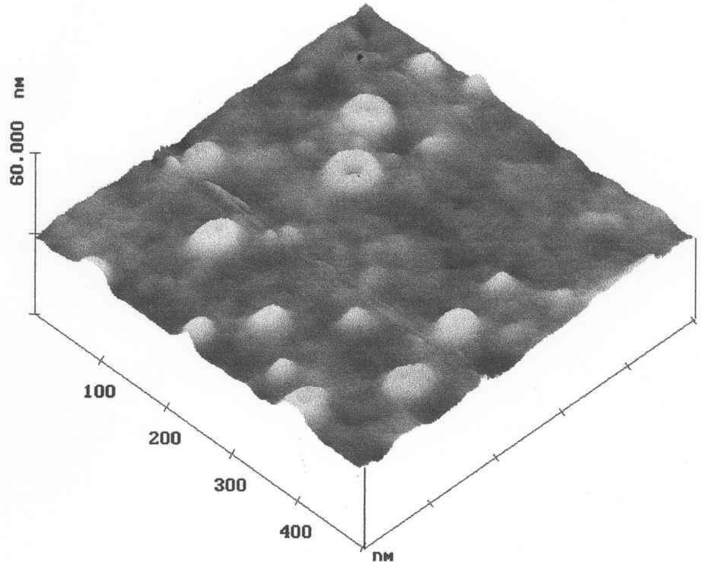

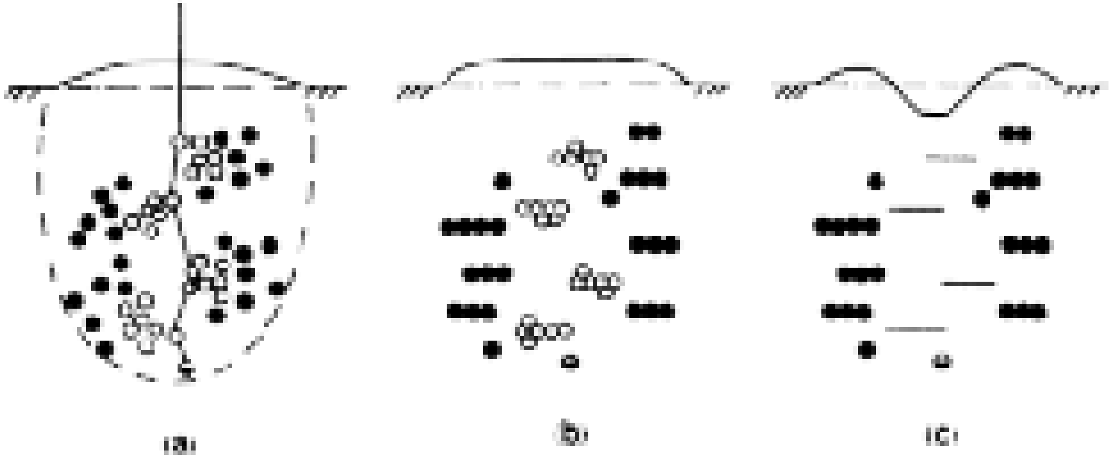

0.5 MeV Ge^+ in (4nm) SiO_2/Si(100)

Dose 5×10^9 ions/cm², 1.85 craters/ion ***I. H. Wilson et al, Phys. Rev. B38 (1988) 8444.***

Craters formed by 0.5 MeV Al ions in GaAs

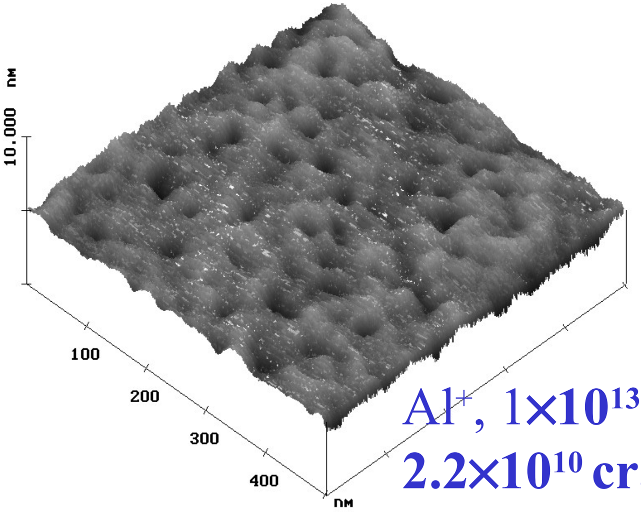

Al^+, **1×10^{13} ions/cm²**

2.2×10^{10} craters/cm²

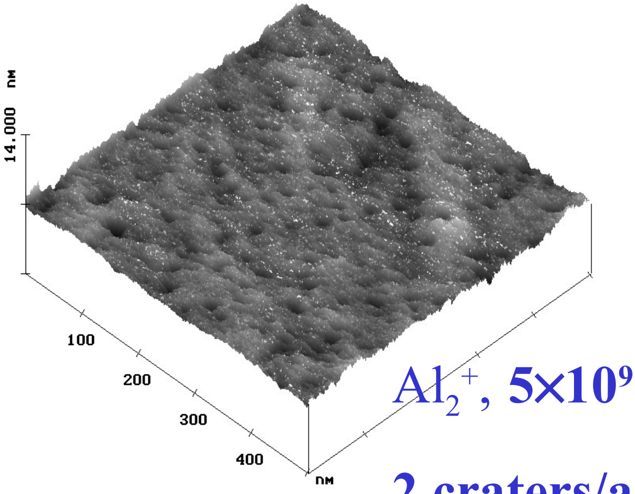

Al_2^+, **5×10^9 ions/cm²**

2 craters/atom

Annealing of craters

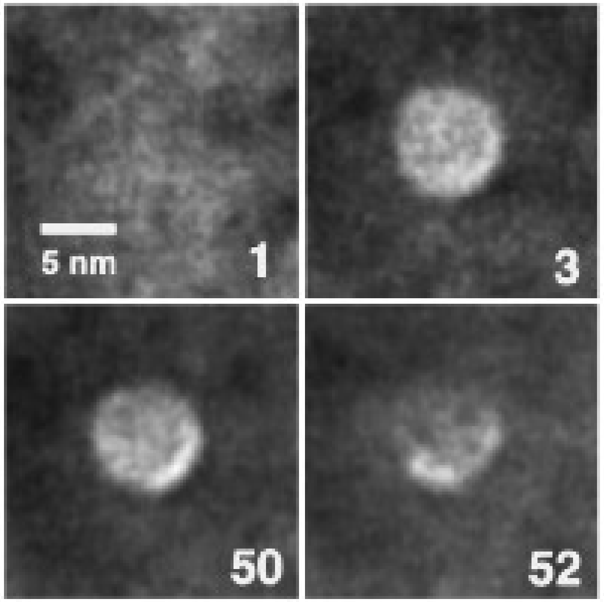

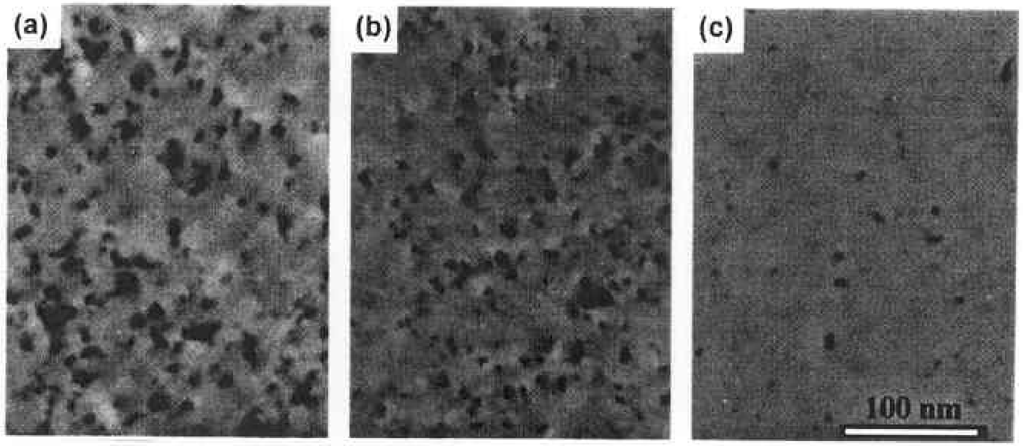

M. W. Bench et al, J. Appl. Phys. 87 (2000) 49

Damage left after 5min, 8 hr, 15days in GaAs/80 keV Xe

S. E. Donnelly, R. C. Birtcher, Phys. Rev. B56 (1997) 13599.

Creation and annihilation of a crater due to impacts of 400 keV Xe ions on Au at various time steps(1/30 s).

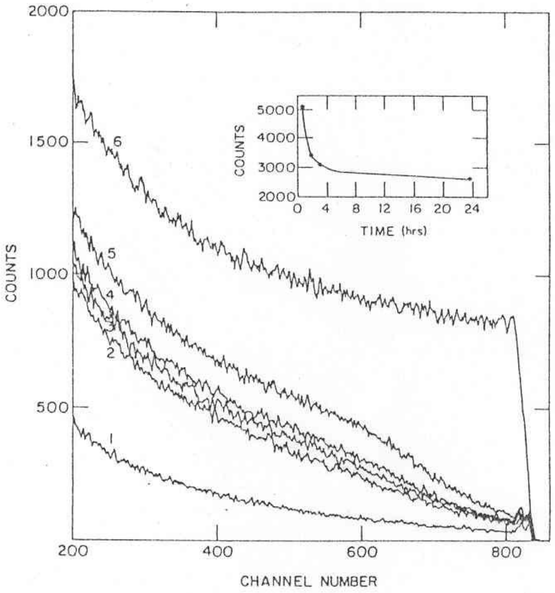

R. P.Sharma et al, J. Appl. Phys. 66 (1989)

3×10^{13} Kr in GaAs (100), Spectra after 0.5, 1.75, 3, 24 hrs.

Evolution of Surface Morphology with dose (Al-dimer in GaAs(100)

1 MeV/atom

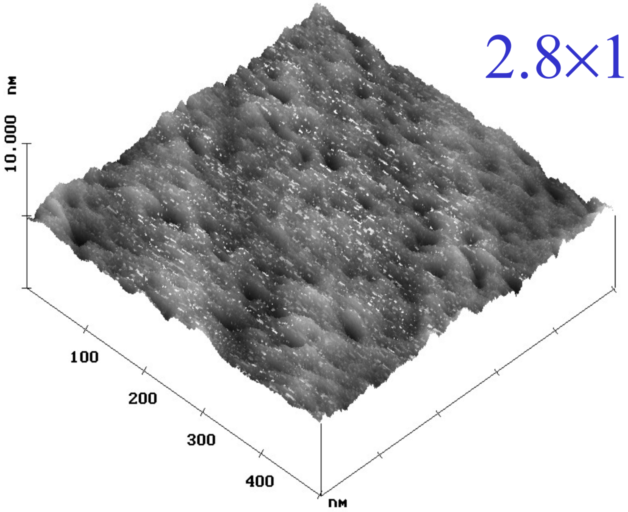

2.8×10^{10}

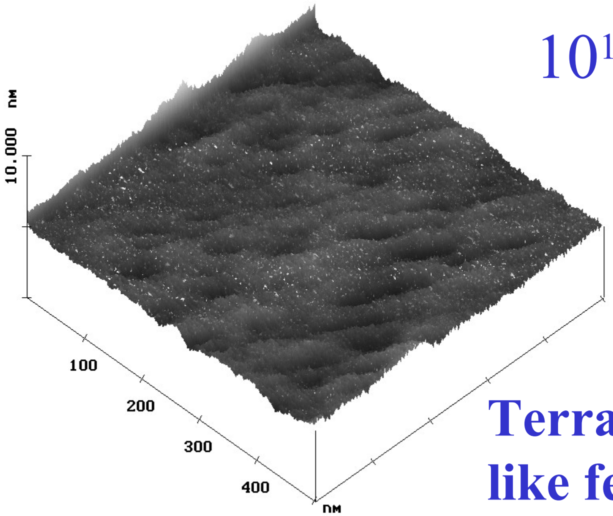

10^{11}

Terrace and canal like features

10^{12} atoms/cm^2

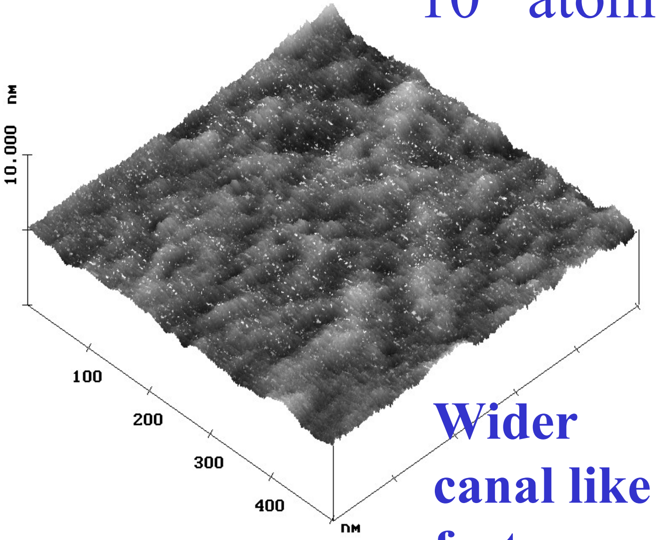

Wider canal like features

10^{13}

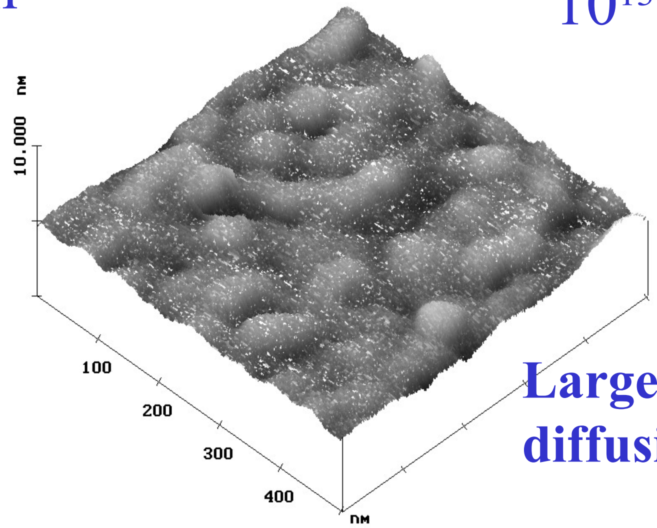

Larger surface diffusion

- **$dE/dx|_e \propto (Z_1 e)^2$**

- **Effective charge of the incident ions approaches the nuclear charge $Z_1 e$ at small and the ion charge $q_1 e$ at large impact parameters.**

- **Channeled ions in a crystal have large impact parameter and the charge state will remain nearly frozen.**

- **Under this condition, $dE/dx|_e \propto (q_1 e)^2$**

- **Also a reduction factor has to be multiplied as there is drop in electron density in the target along a axial direction.**
J. A. Golovchenko et al, Phys. Rev. B23 (1981) 957

- **We have studied the charge state dependence of energy loss of carbon dimer ions in GaAs**

Energy loss of dimer ion

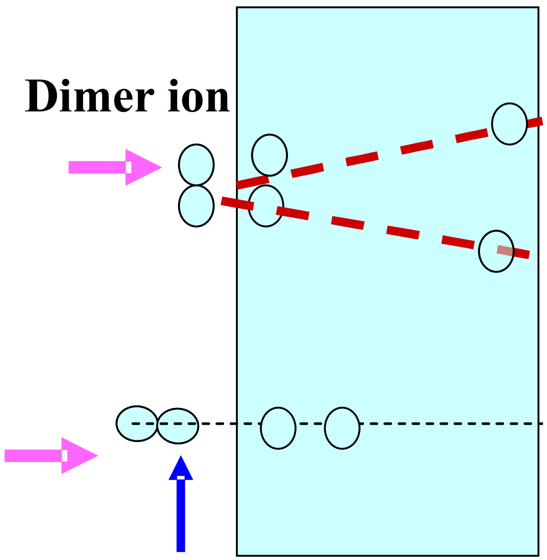

Orientation Effects :

$$R = \frac{S_{\mathrm{cl}}(v)}{\sum_{i=1}^{N} S_i(v)\big|_{\text{ion-beam}}}.$$

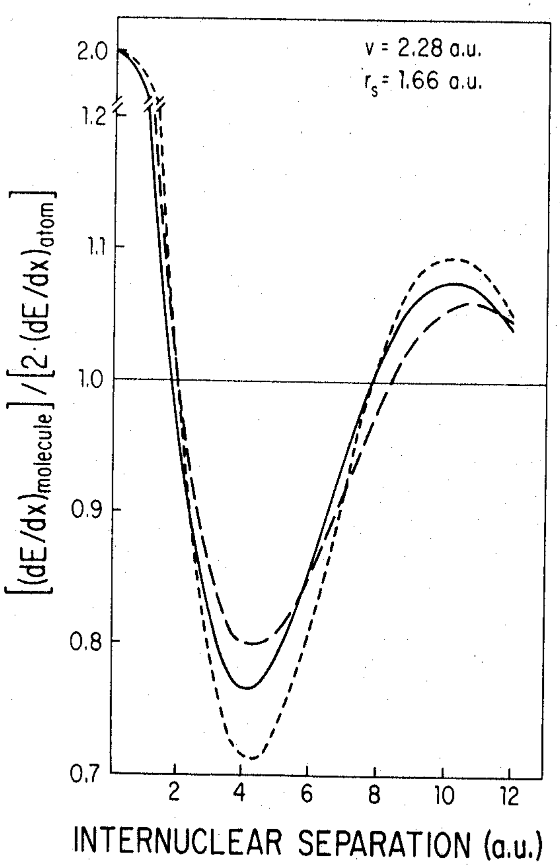

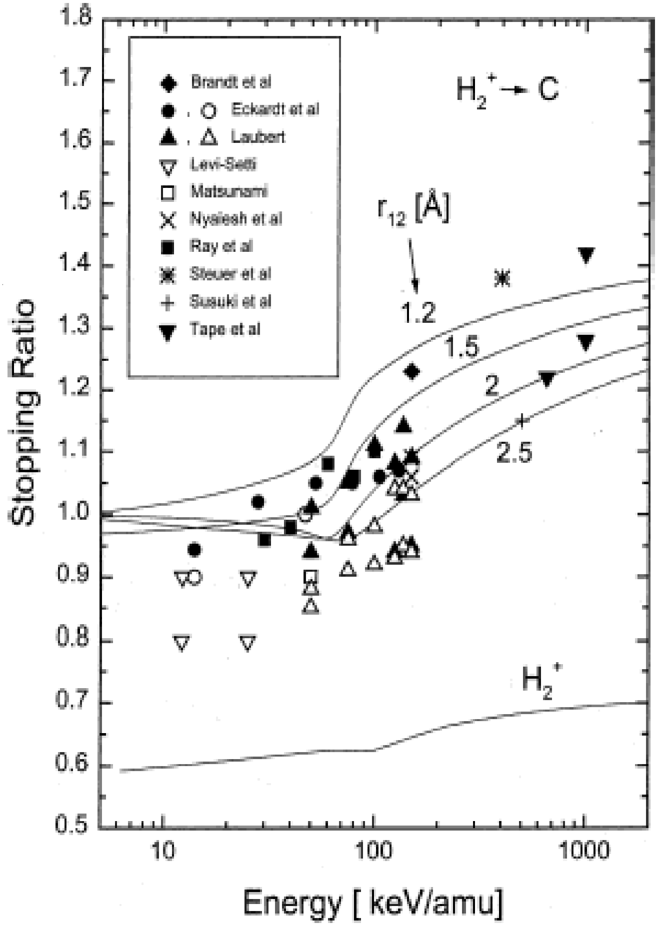

- **Nonlinearity in energy loss of cluster ions, depend on r_{12}, E and orientation.**

- **Energy loss due to change in q_1 in cluster ion is not known.**

Channeling implanation of C_2 and O_2 in GaAs

- **Nonlinearity in sputtering, cratering, lattice damage, energy loss**

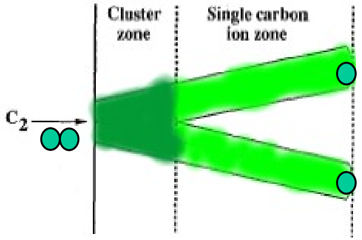

$S_c = S_1 + S_2 + \Delta S_1 S_2$

$\Delta t = r_{12}/v$

$$\Delta \chi(z) = \frac{n_D(z)}{n} + \int_0^z \sigma_D \, n_{D(z')} \, dz'$$

- **Channeling implantation of C_2 & O_2**
- **Negative vicinage effect**
- **Higher damage for dimer**
- **1st report $S_c[O_2{}^{3+}] < S_c[O_2{}^{1+}]$**

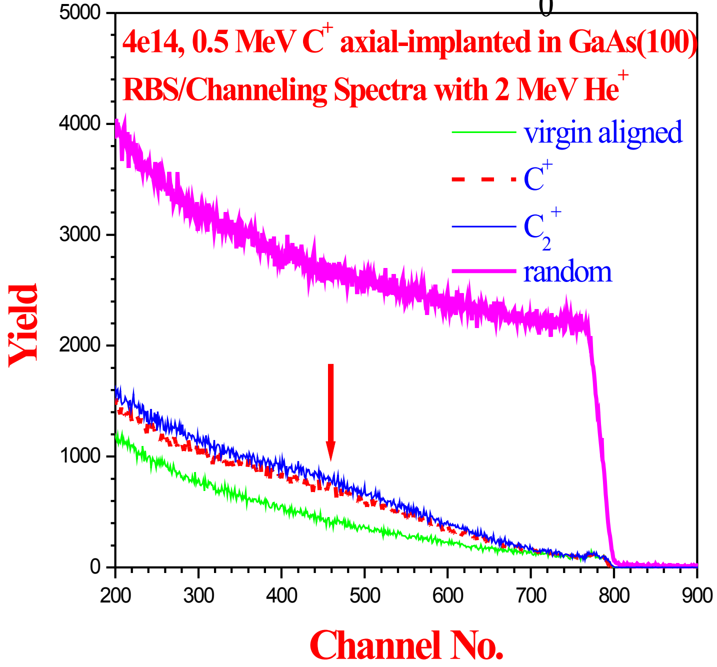

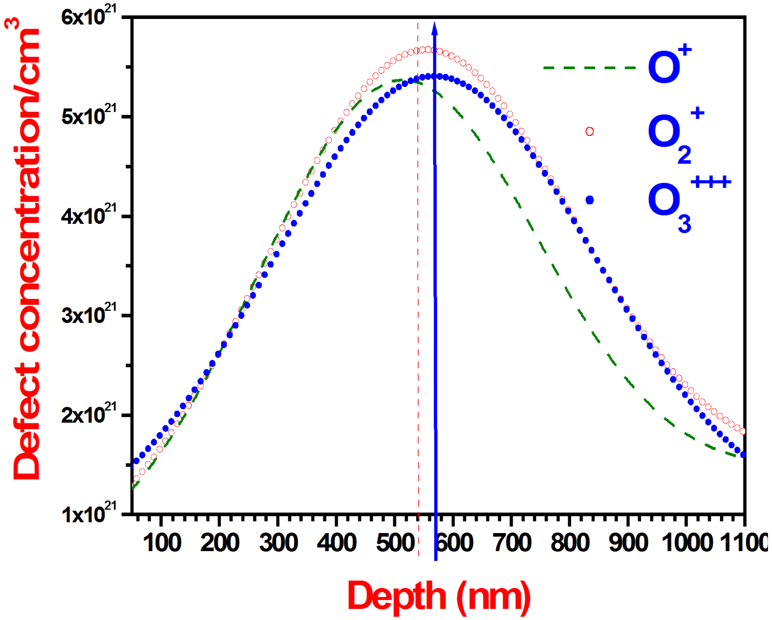

B. Sundaravel et al Phys. Rev. A73 (2006) 042902

At 0.5 MeV/atom, $v=1.29v_0$ for C, 1.12vo for O, r_{12} ,$\hbar/2mv< r_{12} < v/\omega_p$

(behave as separate ions w.r.t. to the closest interactions,united ions w.r.t. the most distant collective interactions) ***N.R. Arista, NIM B 164-165, 108 (2000)***

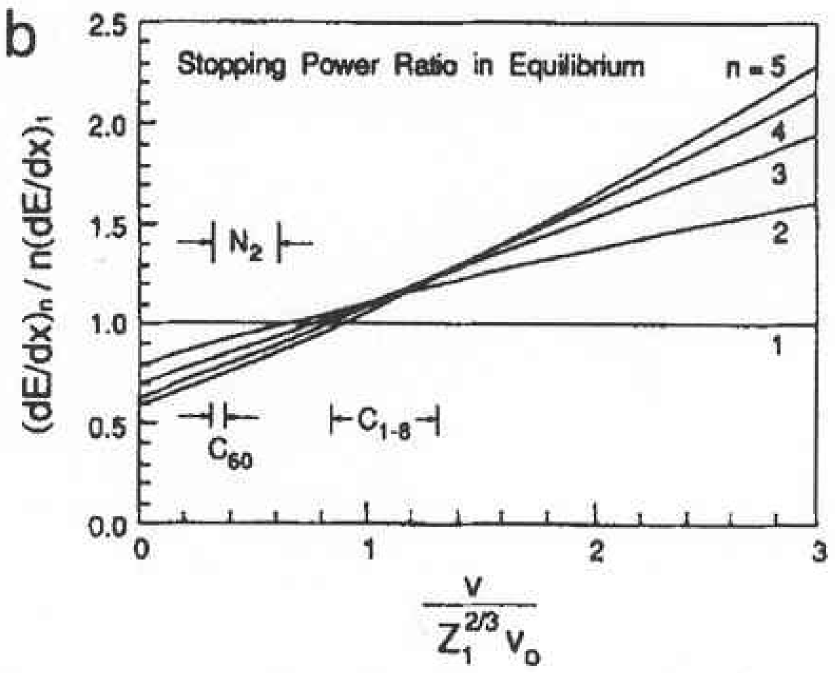

At $r_{12}=0$, TF v= 0.39, 0.28 for C,O, R=0.91, 0.88 for C,O.

P. Sigmund et al, NIMB 196 (2002) 100

So, Negative molecular effect is expected

r_{12} in C_2, O_2 is between $2a_0$ and $3a_0$ (Bohr radius a_0 = 0.0529 nm) and r_{12} for O_2^{+++} is smaller than that of O_2^{+} and O_2^{++} .

Wake field can align the internuclear axis with the beam direction ***D. S. Gemmell et al, Phys. Rev. Lett. 34 (1975) 1420.*** **Channeling can preserve the alignment. Preferred alignment for O_2^{+++} can cause deeper penetration.**

Cluster stability by varying velocity

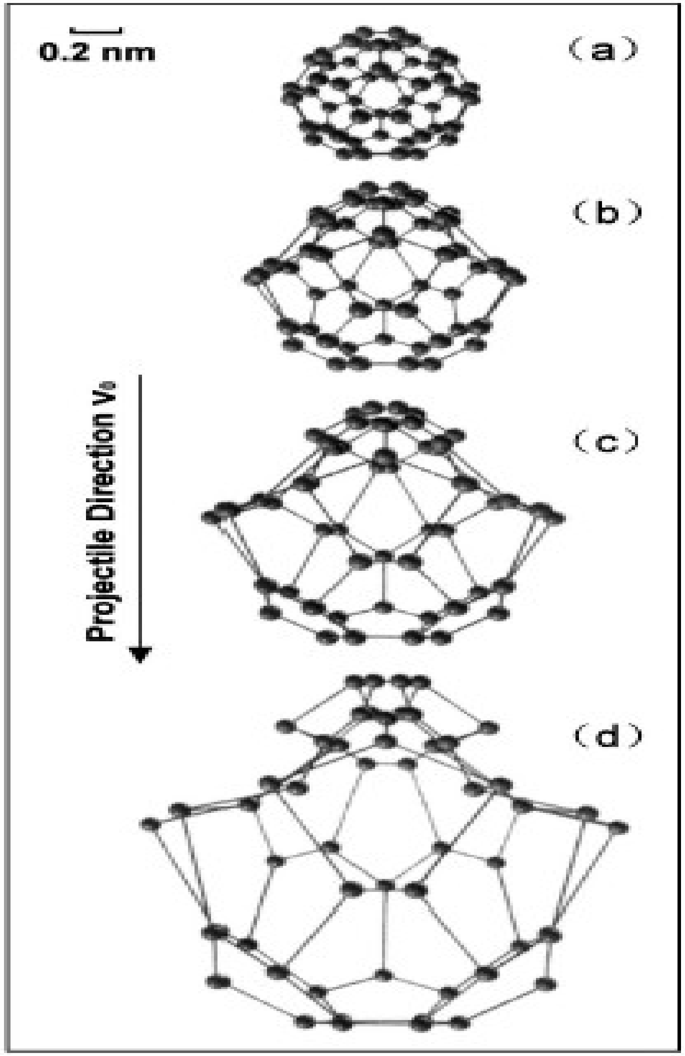

FIG. 2. 3D Coulomb explosion patterns of C_{60} moving through an Al target at speed $v_0 = 4v_B$ in the indicated direction. Snapshots of ion positions are given in a frame of reference attached to the cluster, for several penetration times: (a) $t = 5$ fs, (b) $t = 10$ fs, (c) $t = 15$ fs, (d) $t = 25$ fs.

Y.N. Wang et al, Phys. Rev. Lett. 85 (2000) 1448

12 KeV C-60 fullerene beam on Graphite with benzene layer, M. Kerford and R. P. Webb, NIMB 180 (2001) 44.

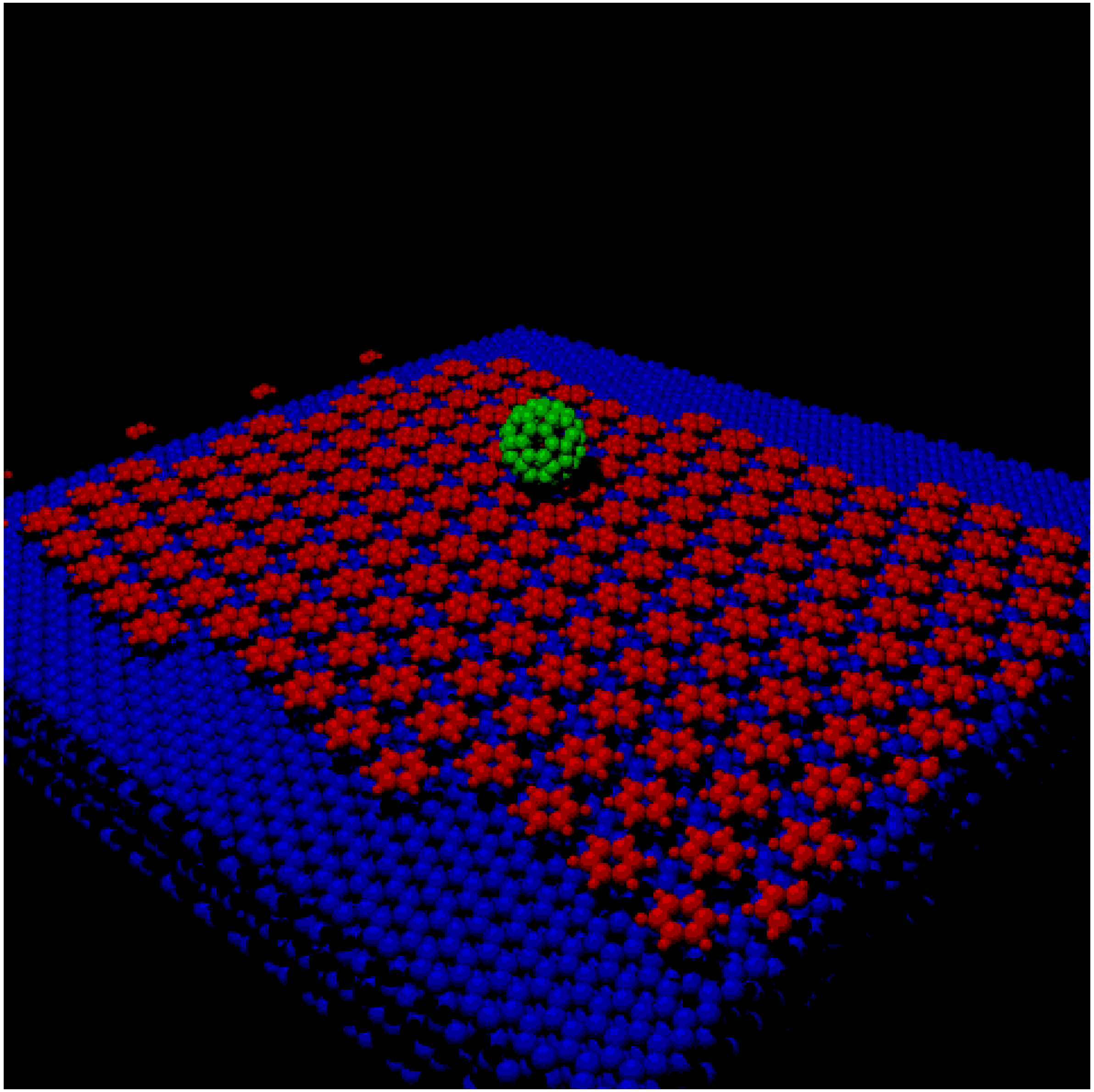

12 KeV C-60 fullerene beam on Graphite- sideview